Materials and Design 186 (2020) 108295

Contents lists available at ScienceDirect

Materials and Design

journal homepage: www.elsevier.com/locate/matdes

A review on crucibles for induction melting of titanium alloys

Simbarashe Fashu [a], Mykhaylo Lototskyy [a,*], Moegamat Wafeeq Davids [a], Lydia Pickering [a], Vladimir Linkov [a], Sun Tai [b], Tang Renheng [b], Xiao Fangming [b], Pavel V. Fursikov [c], Boris P. Tarasov [c]

[a] University of the Western Cape, South African Institute for Advanced Materials Chemistry (SAIAMC), HySA Systems Competence Centre, Bellville, South Africa
[b] Guangdong Research Institute of Rare Metals, Guangdong Key Laboratory of Rare Earth Development and Application, Guangzhou, Guangdong, China
[c] Institute of Problems of Chemical Physics of RAS, Chernogolovka, Moscow Region, Russia

HIGHLIGHTS

- Vacuum induction melting has high application potential in comparison to alternative melting techniques.
- Vacuum induction melting of titanium alloys is hindered by a lack of suitable crucibles.
- Suitable crucible must combine low reactivity with Ti melt at T≥1600°C, thermodynamic stability and thermal shock resistance.
- Coating of shock-resistant crucible with material chemically stable towards interaction with Ti melt is a promising solution.
- Crucible coatings have been successfully verified at laboratory scale, but at industrial scale it still poses a challenge.

GRAPHICAL ABSTRACT

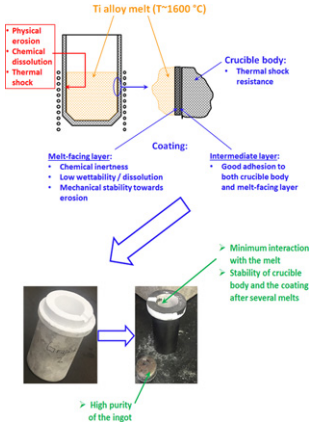

ARTICLE INFO

Article history:
Received 2 July 2019
Received in revised form 18 October 2019
Accepted 19 October 2019
Available online 30 October 2019

Keywords:
Titanium alloys
Induction melting
Crucible
Chemical stability
Thermal shock resistance

ABSTRACT

This review highlights the state of art progress in crucible designs which have been identified as showing potential for induction melting three groups of titanium alloys based on the systems; Ti–Al, Ti–Ni, as well as multicomponent Ti-based hydrogen storage alloys. Several important parameters for crucible design, including; crucible-melt interactions, thermodynamic stability, and, thermal shock resistance of different crucibles will be discussed. Based on the findings of the review, the selection criteria for identifying crucibles for melting titanium alloys were outlined and several specific promising solutions were suggested.

Contents

1. Introduction . . . 2
2. Manufacturing of titanium alloys . . . 3

* Corresponding author.
E-mail address: mlototskyy@uwc.ac.za (M. Lototskyy).

https://doi.org/10.1016/j.matdes.2019.108295

3. Features of titanium alloys related to their manufacturing by induction melting . . . 3
3.1. TiAl alloys . . . 3
3.2. NiTi(X) based shape memory alloys . . . 5
3.3. Hydrogen storage alloys . . . 5
4. Crucible selection criteria . . . 5
4.1. Crucible-melt interaction . . . 6
4.1.1. Physical erosion . . . 6
4.1.2. Chemical dissolution . . . 6
4.2. Thermodynamic considerations . . . 7
4.3. Shock resistance and other factors . . . 9
4.4. Crucible coating . . . 9
5. Crucibles for induction melting titanium alloys . . . 10
5.1. TiAl-based alloys . . . 10
5.1.1. Ceramic oxide crucibles . . . 10
5.1.2. Non-oxide crucibles . . . 11
5.2. NiTi alloys . . . 12
5.3. Hydrogen storage alloys . . . 12
6. Conclusions and perspectives . . . 13
CRediT authorship contribution statement . . . 14
Acknowledgements . . . 14
Appendix A. Supplementary data . . . 14
References . . . 14

1. Introduction

Due to combination of light weight, high strength, excellent toughness, heat and corrosion resistance, titanium and titanium alloys are widely used in a variety of fields, including; the aerospace and automotive industries, manufacture of biomedical components and surgical instruments, chemical and petrochemical engineering, marine applications, etc. [1–8]. Titanium alloys, in particular those based on TiAl, have superior specific strength-temperature properties in comparison to steels and nickel based super alloys in the temperature range 500–900 °C.

The unique properties of certain compositions of Ti-based alloys, for example shape memory alloys [9,10], or hydrogen storage materials [11–14] enable their use in a number of special applications including green power, energy storage, robotics, telecommunication, medicine, etc.

Development of industrial-scale processes for the manufacturing of metallic titanium and its alloys is one of the main priorities of technology development in South Africa [15–19], which possesses 7.9% of global reserves of titanium ores and is the top country (21% of world total in 2017) for their mining [20].

According to data released by the US Geological Survey [20] in 2017, the reservation of ilmenite in China is 200 million tons, or 29% of the global reserves. The sponge titanium production capacity in China by end of 2018 was roughly 110,000 tons, which accounts for 38% of the global total production capacity [21,22]. The priority task of the Chinese titanium industry now is to improve the quality of titanium products, to reduce the production cost, and to eliminate the outdated industrial capacity.

Although titanium alloys have great potential for use in many applications, production volumes are generally low due to the high production costs of the current manufacturing methods. This can be attributed to Ti-based alloys requiring higher processing temperatures (>1600 °C) in comparison to other alloys such as steels (1300–1500 °C) or aluminium alloys (600 °C). At these high temperatures, molten titanium is chemically corrosive to almost any material it comes into contact with, due to its high chemical activity [24]. The high reactivity of Ti-based alloys subsequently makes it extremely difficult to design effective, inexpensive crucible materials to contain the molten titanium during melting. As a result of this, all the current commercial methods for melting titanium utilise power consuming and expensive technologies whereby the molten titanium does not come into contact with any material other than solid titanium. Currently, almost all titanium alloys are melted and cast by vacuum arc remelting (VAR) or induction skull melting using rammed graphite moulds for casting. A typical example of this is the use of a cold crucible for skull melting [25]. Consequently, parts containing titanium alloys are extremely expensive and, as such, their use is generally limited to special and critical applications where the cost factor is almost irrelevant or where no adequate substitution is available. Subsequently, although titanium is the world's fourth most abundant structural metal, in the cast form titanium costs several times more than stainless steel and is about equal in cost to highly alloyed nickel-based super alloys [5].

One approach to overcome some of the processing difficulties experienced with Ti-based alloys is the use of ceramic, refractory metal or graphite crucibles with conventional induction melting to increase the volume of the melt and superheat temperature. This is a promising method for medium-to-large scale manufacturing of castings with the advantages of being simple, allowing for homogeneous stirring of the melt and the ability to maintain a high superheat to enable quality castings to be obtained cheaply at large scale. There are, however, still several challenges which must be addressed before this process can be considered as a long term, commercially viable option and this is mainly due to the high reactivity of molten titanium alloys with the crucible material. The aggressive crucible-melt interaction causes melt contamination, alloy heterogeneity, non-metallic-inclusions and premature crucible failure. Sharp thermal gradients also arise when attempting to reduce the contact time between the melt and crucible, which is the main cause of crucible failure through thermal shock. Determination of how to control the interfacial reactions between titanium melt and crucible materials is, therefore, of great interest.

In 1970, Savitskii and Burkhanov published a comprehensive review considering general features of melting, refining, and casting of chemically active refractory metals and alloys [23]. An overview of early studies on ceramic crucibles suitable for titanium melting was published by Weber et al., in 1957 [24]; oxygen-deficient ZrO_2 was shown to be the optimal crucible material at that time. Developments of ceramic moulds for casting Ti alloys were reviewed by Frueh et al., in 1996 [25]; results of detailed studies of the mould – melt surface interaction were published by the same team a year later [26].

During the last decades, extensive studies to design and develop melting crucibles for induction melting Ti-based alloys at competitive costs have been carried out. Several potential crucible materials have been studied, including nitrides, borides and carbides [27–32],

sulphides [33], ceramic oxides [34–37], graphite and refractory metals [23,38–40]. Stable refractories, including ceramic oxides (such as ZrO_2, Al_2O_3, Y_2O_3, MgO, $CaZrO_3$, $BaZrO_3$) have been identified and some are applied as mould materials for investment casting of titanium alloys [25,34,41–43]. However, identifying suitable crucible materials for induction melting of titanium alloys is still a challenge and, as such, it is not yet commercially practised. Generally, it can be concluded that the lack of adequate crucibles is hindering the large-scale production of titanium alloys.

In order to address these issues, researchers have mainly focused on two aspects of development in this area of research; (i) the production of titanium alloys of quality grade with low contamination level according to the specific alloy requirements [35,44] and (ii) material and design solutions which allow the development of durable/robust shock resistant crucibles capable of melting large volumes of titanium alloys several times [45,46]. Other factors like processability, cost, raw material availability and environmental aspects are also important [46–50]. Subsequently, this article is focused on a systematic state of the art review of crucibles with the potential to be used for induction melting of titanium alloys, explore the challenges being faced, and, show the future direction.

2. Manufacturing of titanium alloys

Current production routes of Ti components are limited to forging [51], powder metallurgy [52] and casting [53]. The disadvantages of forging and powder metallurgy routes are ingot chemical and microstructure heterogeneity, expensive processes and limitations to simple geometries. Another challenge with powder metallurgy is that it can result in oxygen contamination due to open pores. The ingot casting procedure is a promising route to obtain homogeneous and pure alloys at low cost and, further, allows for intrinsic components to be produced.

Vacuum induction melting (VIM) is a commonly used "melting – casting" technique which involves melting an alloy under vacuum or an inert atmosphere by electromagnetic induction using coils (see Supplementary Information, Fig. S1). The main source of power during the process is the alternative magnetic field formed by an alternate current passing through an induction coil. VIM of titanium alloys in refractory crucibles instead of other melting techniques is much less energy intensive [34,35], while at the same time it allows high superheating temperatures, thus improving the cast parts [35,54–56]. In addition, VIM allows fast homogenization of the melt by electromagnetic stirring and is less expensive than alternative melting methods [57,58]. If suitable crucible materials were available, the VIM process would be feasible for large scale component industrial production. Despite its advantages, VIM has not been frequently applied to titanium alloys, largely due to the lack of stable conventional refractory crucibles towards titanium.

Schematic diagrams illustrating various contactless melting techniques are presented in the Supplementary Information, Figs. S2–S5. The advantages and disadvantages of several methods for the melting Ti alloys are summarised in Table S1.

As previously discussed, no suitable ceramic crucible is available for the induction melting of Ti alloys when severe crucible-melt interactions take place at high temperatures. As such, the current practice utilises contactless methods to avoid these interactions. A number of melting techniques can be used instead of melt-contact methods such as vacuum induction melting (VIM).

In arc melting (AM), the alloys are melted under vacuum or an inert atmosphere by an electric arc between an electrode and a water-cooled ground plate (hearth, sometimes also called as crucible, usually made of copper) [59,60]. The electrode may be either non-consumable (water cooled; conventionally made of tungsten) or consumable, made of Ti or Ti alloy. In the latter case, a modification of AM called vacuum arc re-melting (VAR) [59], the electrode material melts at the bottom of the electrode and then falls down accumulating in the melting pool on the hearth to form a new ingot.

AM produces the highest purity ingots. However, the AM process is difficult to upscale and, as a rule, it is used in laboratories to prepare reference samples of the alloys. Another disadvantage of the method is non-homogeneity of the ingot, which requires several remelting procedures and, in many cases, long annealing times [60].

Cold crucible melting (CCM) or levitation melting (LM) which provides suspending of the molten metal by the electromagnetic force [61–63] has recently received considerable attention for the melting of reactive and refractory metals. Induction skull melting (ISM) is a most commonly used CCM/LM technique applied for industrial-scale manufacturing of titanium alloys. It has a unique feature in that the liquid metal is kept in a solid skull of the same metal without contacting the crucible, and is stirred by an electromagnetic force [54,61]. Another modification of CCM/LM is copper boat induction melting (CBIM) [60,62] which uses a water-cooled crucible where the first molten metal immediately solidifies forming a protective layer at the crucible walls. Due to rapid heat loss by conduction from the molten titanium through the solid metal and crucible wall, the power required for melting is high and the amount of molten metal is relatively small. The main disadvantage of the considered methods is that they yield a high level of casting rejections and heterogeneous castings due to low superheat. To overcome these issues mould superheating is necessary, however, this increases contamination and energy costs.

In the industrial-scale processes for Ti melting, CCM is currently used to contain titanium and heating is performed by a central heat source, such as a plasma torch or an electron beam. The extreme thermal gradients in the melt pool allow the outer material to remain solid while the inner molten material is refined and processed. The major problem with using this type of low superheat method is that only a relatively small amount of material can be melted at a time due to skull formation. In addition, the low superheat leads to low fluidity of the melt pool which, in turn, results in a significant waste during casting, heterogeneity of the final product, process misruns and other associated defects. High equipment and energy costs and long cycle times are also typical challenges of the CCM melting technologies.

Besides AM and ISM, advanced melting processes like vacuum plasma spraying [64,65], selective laser melting [66] and electron beam melting [66–68] are also receiving attention due to their capability to produce high quality castings. These methods do not involve the use of crucibles which contact with Ti melt and, therefore, will not be considered later in this review focused on VIM technique.

3. Features of titanium alloys related to their manufacturing by induction melting

Alloys based on the systems Ti–Al, Ti–Ni, as well as multicomponent hydrogen storage alloys are typical representatives of the titanium-based materials whose features greatly impact on the problems of design of melting crucibles considered in this review. The present section briefly considers these types of the alloys illustrated by several binary phase diagrams (Fig. 1) [72].

3.1. TiAl alloys

As a result of high strength-to-weight ratios and excellent mechanical and corrosion properties at high temperatures, γ-TiAl alloys are more studied and are commonly referred to as the "future alloys" to replace traditional Ni, Co and Fe based superalloys and steels for high temperature applications in the automotive, aeronautical and aerospace industries [73–76]. Significant improvements are being made, with the development of new multi-component TiAl-based alloys (typical additives V, Nb, Ta, Cr, Mo, W, Zr [2]) characterised by improved mechanical properties [77,78] and superior oxidation resistance at high temperature [79]. As it can be seen in Supplementary Information, Table S2, typical Ti-48Al alloy is characterised by tensile strength >1.4 times higher than that for mild steels (at >2 times lower density)

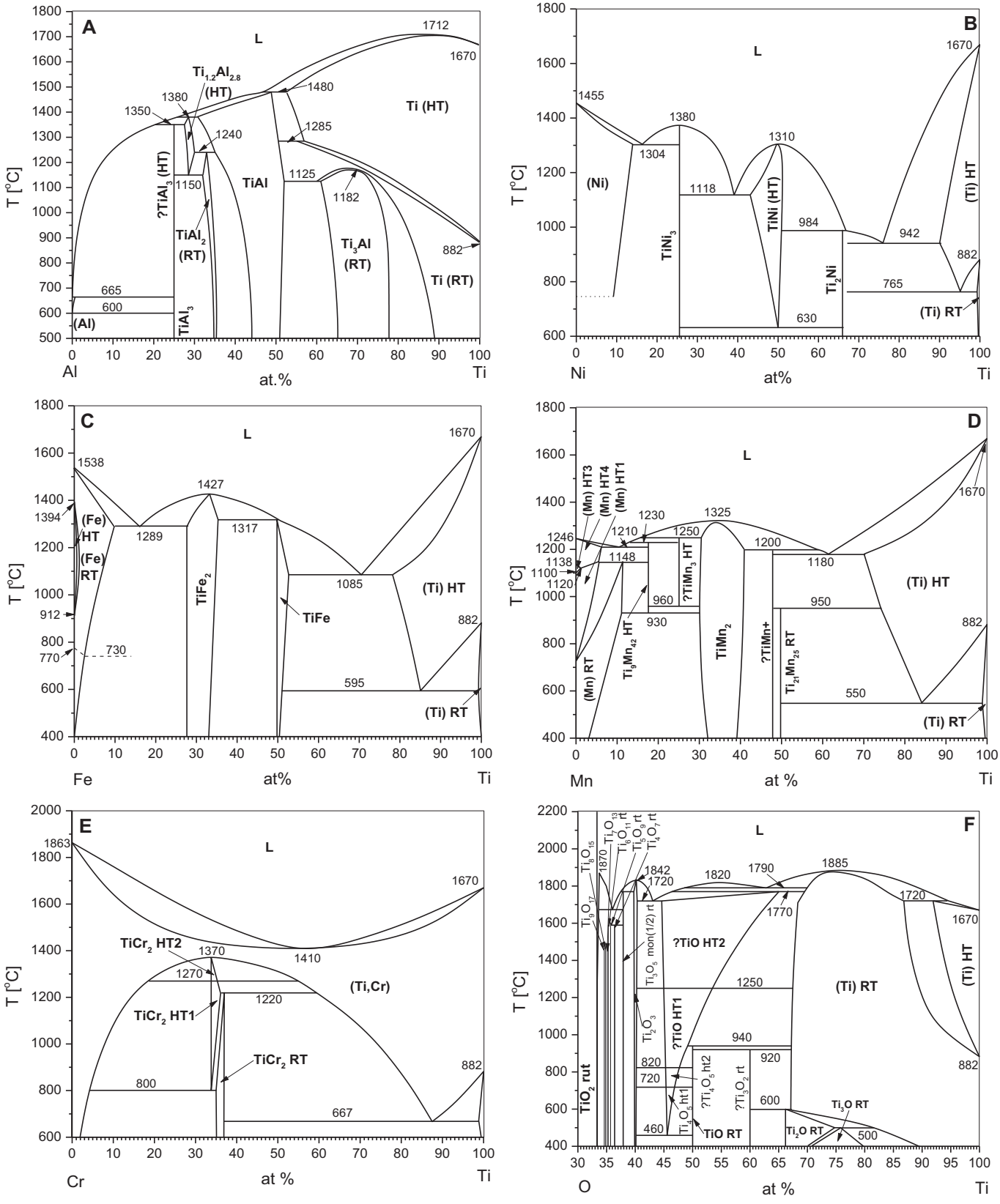

Fig. 1. Equilibrium phase diagrams of Ti systems [72]: Ti–Al (A), Ti–Ni (B), Ti–Fe (C), Ti–Mn (D), Ti–Cr (E) and Ti–O (F).

while the strength of a commercial Ti6Al4V alloy further increases by 49–65%. Further improvement of performance of TiAl-based alloys can be achieved by the introduction of nitrogen which results in the increase of surface strength and refined microstructure [2]. Another important non-metallic additive is hydrogen whose temporary introduction facilitates processing of TiAl based materials via preparation of their powders characterised by high purity and refined microstructure (hydrogenation–decomposition–desorption–recombination/HDDR)

[80]. The hydrogenation can be carried out using gaseous H_2 [81], or by the interaction of the alloy with ammonia [82,83]. In the latter case, the hydrogenated alloy also contains nitrogen which remains in the material after removal of hydrogen thus enabling further control of mechanical properties of the final product.

Two of the commonly used TiAl alloys include TiAl(γ) and Ti6Al4V and their use varies depending on the end application. The aggressiveness of the crucible-melt interactions in VIM depends on the titanium content of the alloy, for example, Ti6Al4V alloys (melting point (m.p.) = 1640 °C) are more aggressive to crucibles compared to TiAl(γ) alloys (45–50% Al; m.p. = 1460 °C), and pure Ti (m.p. = 1668 °C) is even more aggressive. TiAl(γ) alloys can be melted at temperatures between 1550 and 1750 °C, while Ti6Al4V alloys require higher melting temperatures (1660–1800 °C) due to the high Ti content. The equilibrium phase diagram of Ti–Al system ([72]; vol.1, pp.225–227) is shown in Fig. 1A and it clearly demonstrates how the melting point of the alloys drops from that of pure Ti to approximately 1500–1600 °C for TiAl(γ) alloys.

Currently, the main factors limiting the mass manufacture of TiAl-based components are the intrinsic characteristics of TiAl alloys i.e. microstructure and chemical heterogeneity, brittleness, low room temperature ductility and poor hot workability [56], as well as the high production costs. Investment casting is one of the most economical methods for the precise production of titanium and titanium aluminide alloy castings and it has been found to increase the integrity and mechanical properties of components, while at the same time reducing material waste and machining cost [71].

3.2. NiTi(X) based shape memory alloys

Although NiTi-based shape memory alloys have been known worldwide since the 1970s, literature related to their processing is limited, owing to production difficulties. As a result of this there are very few NiTi producers in the world. NiTi shape memory alloys (SMA's) are the most successful SMA's today because they combine good functional properties with high mechanical strength [84–87]. Shape memory (SM) properties are strongly dependent on alloy composition and, therefore, it is critical to produce alloys with good chemical homogeneity. It is known that a difference of 0.1 at.% in Ni-content results in a 10 °C difference in phase transition temperatures [88,89]. Elements like Cu, Hf, Pt, Pd, Nb, Au and Zr are often added to NiTi alloys to form ternary shape memory alloys with improved properties [87]. During VIM, ternary alloys can be prepared in two steps; by first melting the binary alloy and then adding the third element. The melting point of Ni50Ti is ~1310 °C (Fig. 1B, [72]; vol.3, pp.2874–2876) so melting is generally performed between 1450 and 1500 °C. These melting temperatures are lower than those required for melting TiAl alloys (1500–1600 °C; Fig. 1A), and, therefore, crucible-melt reactions are less aggressive so there is less challenge in identifying suitable crucible materials for Ni50Ti alloys.

3.3. Hydrogen storage alloys

Hydride forming hydrogen storage materials are represented by a large number of multicomponent composites and alloys. The latter group, which includes intermetallic compounds and solid solution alloys which are able to reversibly interact with hydrogen, is important for a number of applications including compact hydrogen storage, hydrogen compression and heat management, nickel – metal hydride rechargeable batteries [90–102].

Ti-containing hydrogen storage materials are mainly represented by intermetallic compounds $TiFe_{1-x}M_x$ (structure type CsCl; M = Mn, V) [97,103,104], Ti_2M (structure type Ti_2Ni, M = Fe, Co, Ni) [105,106], body-centred cubic (BCC) solid solutions on the basis of Ti–Cr and Ti–Cr–V systems [98,99] and Laves phases of general composition $AB_{2\pm x}$ where A = Ti + Zr, B═Mn, Cr, V, Ni, Fe and other metals [13,14,107]. Two latter types of Ti alloys, particularly C14-type Laves phases on the basis of Ti–Cr–Mn system, are of special importance since their hydrides are characterised by high dissociation pressures and can be used in "hybrid" hydrogen storage and hydrogen compression applications [14,100,101]. An important feature of these materials, in particular for AB_2-type alloys, is the possibility of significant variation of properties related to their interaction with hydrogen by modification of the component composition, which enables the development of specific recipes/compositions to meet the demands of various end-use applications. At the same time, this feature poses a strict requirement to avoid deviations from the target alloy composition (less than 3–4%). The homogeneity of the final product is also an important consideration. To achieve compositional homogeneity, as-cast alloys are typically subjected to heat treatment or rapid quenching [11]. The hydrogen storage properties of Ti-based alloys are also very sensitive to non-metallic impurities [102], particularly oxygen [103,108], and deoxidisers (rare-earth metals) are recommended to be added during their melting to negate this effect [109].

Phase diagrams of typical binary systems of titanium, in which hydrogen storage intermetallics are formed, are shown in Fig. 1C [72]; vol.2, pp.1783–1786 (Fe–Ti; hydride-forming intermetallic $Ti_{1+x}Fe$, x = 0.0.05), Fig. 1D, [72]; vol.3, pp.2615–2617 (Mn–Ti; hydride forming intermetallic $TiMn_{2+x}$, x = −0.56.0.33) and Fig. 1E, [72]; vol.2, pp.1345–1348 (Cr–Ti; 3 allotropes of hydride forming intermetallic $TiCr_{2-x}$, x = 0.06.0.3). The solidification at these compositions takes place below 1317 °C, 1325 °C and 1535 °C for TiFe, $TiMn_{2+x}$ and $TiCr_{2-x}$, respectively. Taking into account the coexistence of $TiFe_2$ in the Ti–Fe system (solidification at 1417 °C; does not form hydride at reasonable conditions [103]), the melting pool for the preparation of TiFe has to be at temperatures above 1500 °C, and melting of AB_2-type alloys requires temperatures above 1600 °C, similarly to TiAl alloys.

Many multicomponent Ti-based alloys used for hydrogen storage and other applications, particularly Laves phases and/or BCC solutions, often contain components characterised by melting points significantly higher than that of pure titanium (m.p. = 1668 °C), for example, chromium and zirconium (m.p.>1850 °C), vanadium (m.p.>1900 °C), niobium (m.p.>2400 °C) [14,61,65–70]. Thus there exists a possibility that the melting temperature of these alloys will be higher than 1600 °C[1] that poses additional challenges in crucible selection.

The high melting temperatures and sensitivity of hydrogen sorption performances of TiFe and Ti-based AB_2-type alloys to contamination and inhomogeneities [11,14,102–108], results in challenges in alloy production through induction melting. In order to minimize the contact time between the crucible and the aggressive components in the melt at high temperature, it has been suggested to pre-alloy the less aggressive components (e.g. Mn with FeV), further co-melted with other metals which are more aggressive (rare-earth metal deoxidiser) or more refractory (titanium, zirconium, chromium) [109]. Large metallurgical companies prefer to melt Ti- and Zr-containing AB_2-type hydrogen storage alloys in large capacity (>1000 kg/load) crucible-free plasma-heated skull furnaces [11]. However, due to economic reasons, their product line is limited to a few compositions, and the variation of component composition of the target alloy (that is necessary for different end-use applications) is, therefore, limited.

4. Crucible selection criteria

In order to commercially use induction melting for the large scale production of titanium alloys, the melting crucible should be carefully selected and designed to avoid melt contamination [110]. The procedure for selecting, and further, designing potential candidate crucible materials for melting a particular titanium alloy involves consideration of several important aspects, including; crucible-melt interaction and

[1] According to practical experience of the authors, the melting of a multicomponent $Ti_{0.85}Zr_{0.15}Mn_{1.2}M_{0.8}$ (M = V + Cr + Ni + Fe) AB_2-type hydrogen storage alloy (see section 5.3 below) takes place at 1650–1700 °C.

thermodynamics of the reactions involved, melting and softening temperatures, wettability, and thermal shock resistance.

4.1. Crucible-melt interaction

Generally, interactions between a ceramic crucible and molten metal include chemical reactions and physical erosion. In such a situation, erosion will complement chemical attack by removal of the reaction products from the surface to expose fresh surfaces and facilitate further chemical attack.

4.1.1. Physical erosion

During melting, when the metal reaches the liquid state and its fluidity is high enough, if good wetting exists between the melt and the crucible, the melt can penetrate into the crucible by capillary forces and attack the grain boundaries (Fig. 2). Refractory particles can, therefore, be more easily entrained into the melt by mechanical action, particularly electromagnetic stirring [34,41,55,111–113].

Fig. 2 schematically illustrates this process; the dashed arrow in Fig. 2 (left) shows removal of a particle from the crucible body into the melt due to erosion. As a result (Fig. 2 (right)), the entrained particle becomes completely surrounded with the melt promoting further chemical dissolution (see next section) due to increase of the "melt – crucible material" contact area (red lines), as well as facilitation of mass transfer in the melt not restricted anymore by the conductivity of channels filled with the melt in the porous crucible body. On the other hand, removal of the particle results in the channel expansion (pink background) thus facilitating further penetration of the melt in the pores. Finally, it promotes further entrainment of neighbouring particles (circled in Fig. 2 (right)) into the melt due to weakening of their bonding with the crucible body.

The extent of erosion depends on the convection force applied to the crucible surface and is high when high induction power is used in order to achieve higher superheat and strong stirring. The eroded ceramic particles may either be dissolved or survive in the melt, depending on holding times and superheats. Erosion occurs because refractory crucibles normally contain a controlled amount of porosity which is intentionally left to improve their resistance to thermal shock. The distance of melt penetration into the crucible (L; Fig. 2) at the crucible-melt interface is related to the pore radius (r), surface tension of the molten alloy (σ), the melt-crucible wetting angle (θ), the viscosity of melt (η), and, interaction time (t) according to Equation (1) [112].

$$L = \sqrt{\left(\frac{r\sigma\cos\theta}{2\eta}\right)t} \tag{1}$$

Equation (1) shows that a large crucible pore size, wettable crucible surface, high melt surface tension, less viscous melt and long interaction times cause deeper melt penetration into the crucible. Using sessile drop tests, Lopez and Kennedy [114] studied the wetting behaviour on ceramic substrates and the result showed that the wetting process is a thermally activated process. The drop spreading rate follows the Arrhenius equation (2):

$$\frac{dr}{dt} = k\exp\left[\frac{-E_a}{RT}\right] \tag{2}$$

where, r is the radius of the drop, t is the measured time, dr/dt is the speed of sessile drop spreading, k is a pre-exponent, E_a is the spreading activation energy, R is the gas constant, and T is the operation temperature (K).

The key to reducing physical erosion is to optimize porosity, which leads to good erosion resistance and shock resistance, but this is difficult to achieve. In addition, the holding time and superheat during melting should be optimized to minimize melt infiltration into the crucible.

4.1.2. Chemical dissolution

As the alloy starts to melt in the crucible, it reacts with the crucible and dissolves the constituents of the crucible into the melt. For an Y_2O_3 crucible, the dissolution reaction is

$$Y_2O_3(S) \leftrightarrow 2Y(L) + 3O(L) \tag{3}$$

where, L means molten TiAl.

The presence of electromagnetic stirring in the melt and high diffusion rates of solutes in the superheated liquid ensure a uniform distribution of contaminants in the molten alloy. For particles that are eroded and dispersed into the melt, the contact area between the particles and the melt which completely surrounds every particle is increased, thereby promoting a high dissolution rate. The melt contamination generally increases with an increase in superheat and melt holding time in the crucible. This effect is more severe for larger crucibles compared to

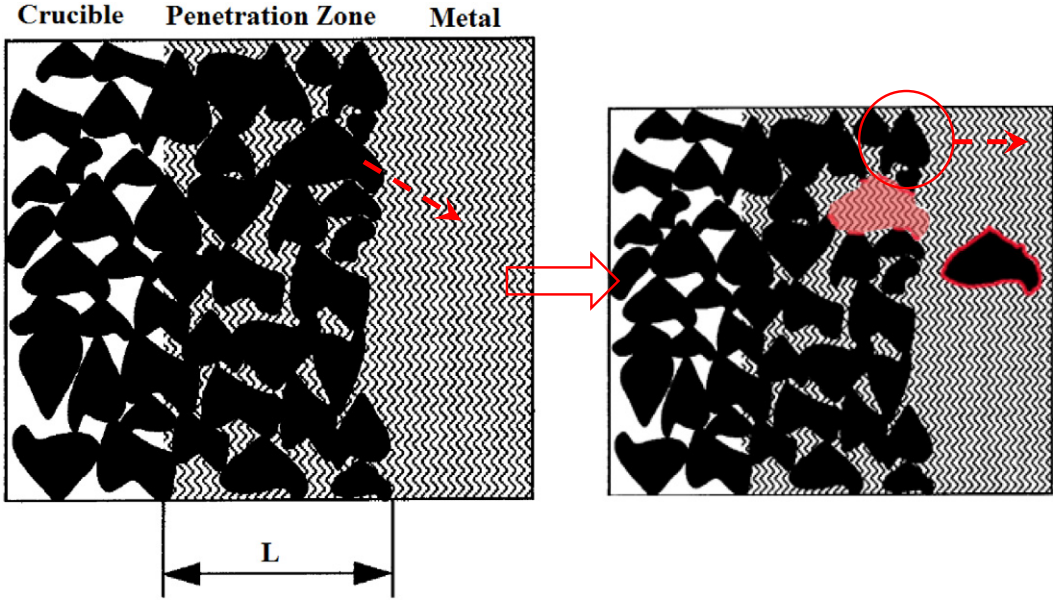

Fig. 2. Schematic diagram of melt penetration into crucible and entrainment of the crucible particles into the melt. Adapted from Ref. [34].

smaller crucibles since large crucibles require longer holding times for homogenization. If the sample is allowed to solidify inside the crucible, the interaction between the crucible and melt continues at the interface through dissolution controlled by diffusion, which results in composition gradients between the surface and the bulk. Interaction layer thicknesses, shown in Table 1 and Table 2, are likely to be established more during solidification inside the crucible rather than during melting, because during melting most reaction products are eroded into the melt due to mixing. Nearly all ceramic crucibles are attacked by molten titanium to some extent and this includes the known thermodynamically stable Y_2O_3 [34,41,55,111–113] and CaO [76,115] oxides. For TiAl alloys, Y_2O_3, $BaZrO_3$, Ca-Doped $BaZrO_3$ and AlN showed the lowest oxygen content in the ingot and meet the specification of <0.1 wt % oxygen. In NiTi (-X) alloys, Table 2 shows that $BaZrO_3$ and high density graphite crucible are suitable materials for melting the alloys.

4.2. Thermodynamic considerations

Thermodynamic considerations involve a comparison of the free energies of formation of refractory compounds with the corresponding titanium phases and are dependent on the alloy being melted (e.g. TiO, TiO_2, TiN, TiB_2 and Ti). Based on this approach, any compound which has a more negative free energy of formation than the appropriate titanium compound at a particular operating temperature would be identified as a candidate.

Fig. 3A shows Ellingham plots of the standard free energy for the formation of selected binary oxides and that of TiO which is in equilibrium with molten titanium [135,136]. The general reaction for oxides formation represented on the diagram is:

$$\frac{x}{y}M(S,L\text{ or }G)+\frac{1}{2}O_2(G)\rightarrow\frac{1}{y}M_xO_y(S,L\text{ or }G) \quad (4)$$

where M is the metal element, O is oxygen, x and y are the stoichiometric coefficients.

We note that while in the reference literature (see e.g. Ref. [137]) the Ellingham diagrams are presented as temperature dependencies of standard Gibbs free energy of formation of 1 mol M_xO_y, the comparison is correct when all oxide formation reactions are normalised to consume 1 mol of oxygen [138]. For convenience, we use the values per one g-atom of oxygen, or mole $^1/_2$ of O_2, so as the reference value of ΔG_f^0 [kJ/mol] for the oxide, when presented in Fig. 3A in kJ/g-at O, should be divided by stoichiometric coefficient y as shown by Reaction (4).

It can be seen that CaO and Y_2O_3 are potential crucible materials for direct melting of Ti because their free energies are more negative at all temperatures whereas SiO_2, MgO and Al_2O_3 have ΔG_f^0 [kJ/g-at O] which is less negative than that of TiO [47,110,135] at $T \geq 1600$ °C; therefore, they cannot be directly used for melting. The suitability of ZrO_2 requires more detailed thermodynamic consideration because its free energy of formation (per 1 g-at. O) is very close to the one for TiO.

A disadvantage of the oversimplified thermodynamic approach, which only takes into account the stability of the crucible material (e.g. oxide; Reaction (4), compared to the stability of TiO (Fig. 3A)), is that it does not consider specific features of the interaction of the melt with the crucible material. As can be seen from the phase diagram for binary oxygen–titanium systems [72]; vol.3, pp.2924–2927 (Fig. 1F), oxygen has very high solubility in Ti and forms a large number of suboxides in addition to TiO. This means that the thermodynamics of interaction of a Ti melt with oxygen bound in the crucible material may strongly depend on the oxygen concentration in the melt or product of its solidification. Similar behaviour is exhibited by several other systems, e.g. O–Zr [72]; vol.3, pp.2940–2941. Additional complications can also be introduced by the presence of other alloy components, which can significantly alter the thermodynamics of the melt – crucible interaction.

A detailed consideration of the interaction thermodynamics between Ti–Al(–V) melts and a number of binary and mixed oxides as candidate materials for making crucibles was performed by Kostov and

Table 2
Summary of the reported literature data on contamination of NiTi(-X) alloys during vacuum induction melting in different crucibles.

Crucible	Interaction Time/min	Interaction Layer Thickness/μm	Contamination Level/wt%	References
SiC	90	[a]	C:1.129	[27,32]
Al_2O_3	90	[a]	O:1.6	[27,32]
ZrO_2	90	[a]	O:1.046	[27,32]
$CaZrO_3$	5	30	–	[123]
$BaZrO_3$	2	20	O:0.065–0.09	[126]
High Density Graphite	0.2–49	2–5	O:0.02–0.082 C:0.017–0.25	[38,39,44,130–134]

[a] Data not reported.

Table 1
Summary of the reported literature data on contamination of TiAl alloys during vacuum induction melting in different crucibles.

Crucible	Interaction Time/min	Interaction Layer Thickness/μm	Contamination Level: wt%	References
SiO_2	0.5–5	[a]	O:1.7, Si:1.7	[36]
Mullite ($3Al_2O_3{\cdot}2SiO_2$)	15–60	190–840	-	[41]
MgO	18–60	1296–3570	O:0.95–1.09	[34]
Al_2O_3	0.5–60	30–247	O:0.16–2.5	[34,36,37,41,45,115–117]
ZrO_2 (incl. stabilized)	0.5–60	120–300	O:0.55–1.29	[36,41,45,48,116]
Y_2O_3–$15ZrO_2$	3	[a]	O:0.38	[36]
CaO	0.5–60	5	O:0.10–0.71	[34,35,45,48,115,116]
Y_2O_3	0.5–60	8–100	O:0.06–0.33	[17,41,45,73,113,115,116,118]
Y_2O_3-coated MgO	18–60	10–19	O:0.016–0.21	[34]
Y_2O_3-coated Al_2O_3	10–34	[a]	O:0.04–0.13	[84,119]
Y_2O_3-coated ZrO_2 (incl. stabilized)	60–120	15–65	O:0.21–0.31	[55,120–122]
Y_2O_3-coated $ZrO_2{\cdot}SiO_2$	1	[a]	O:0.19–0.22	[49]
$CaZrO_3$	5–20	300–350	O:0.13–0.73	[57,123,124]
$CaZrO_3$- Al_2O_3 Composite	30	150	–	[125]
$BaZrO_3$	5	870–2000	O:0.065–0.13	[126,127]
Ca-Doped $BaZrO_3$	2	5	O:0.09	[128]
AlN	5–25	1.1–6.4	O:0.025–0.113	[27]
BN	5–25	250->500	–	[27]
Graphite	0.3–2	[a]	C:4	[48,129]
Water cooled Cu	3	0	O:0.09	[36]

[a] Data not reported.

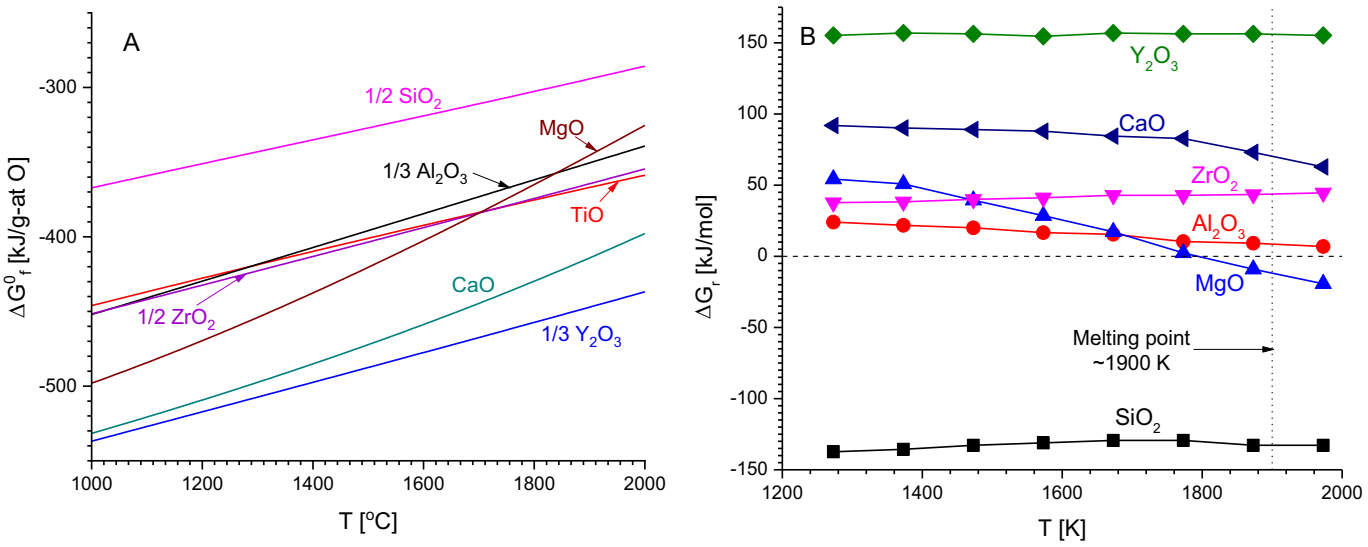

Fig. 3. Temperature dependencies of Gibbs free energy of: A – formation of different binary oxide refractories; B – reaction of selected crucible materials with TiAl6V4. The presented data have been adapted from Refs. [110,135].

Friedrich [110,135]. Special attention was paid to the activity – temperature relationships for free energy change of reactions for the selected ceramics with Ti alloy melt. It was concluded that out of six binary oxides (CaO, Y_2O_3, ZrO_2, MgO, Al_2O_3, SiO_2) and several of their combinations (oxide spinels), only CaO, Y_2O_3, ZrO_2 and Al_2O_3 have positive values of free energy, ΔG_r, in respect to their interaction with Ti–Al(–V) at $T = 1273$–1973 K in the whole range of Ti concentrations (see example in Fig. 3B). However, for the alloys characterised by high Ti concentrations and high melting temperature, ΔG_r for Al_2O_3 is close to zero which is problematic for its use in crucible making.

The thermodynamic stability of multicomponent systems containing liquid and solid phases can be also calculated using real or hypothetical equilibria of these condensed phases with a gaseous phase. On the basis of available reference data on the corresponding phase equilibria, the partial pressures of the components in the gas phase can be calculated under the condition of the minimum of the total pressure (i.e. minimum ΔG) at a given temperature. The oxidation potential of the system will be equal to the sum of partial pressures of oxygen-containing components, as a rule; $(P_o + P_o 2)$ [136].

According to the approach described above, calculations were carried out and verified experimentally for the systems Zr–V [139] and Zr–Fe [140] with the presence of various oxides (Fig. 4). The experimental verifications included arc melting of Zr + V or Zr + Fe mixtures under argon in the atomic ratios 1:1 and 2:1, respectively, with additives of oxide powder (1–20 wt%) followed by XRD analysis. Interaction between the melt and the oxide powder was identified by the disappearance of the oxide phase in the XRD pattern of the alloy, as well as by the formation of η-phases $Zr_3V_3O_{1-x}$ or $Zr_4Fe_2O_{1-x}$ characterised by high stabilities and wide homogeneity regions in respect to oxygen content.

As it can be seen from Fig. 4, the calculated results are in a good correspondence with the experimental data. The additives with a lower oxidation potential, or higher value of $-\lg(P_o)$, than the Zr–V–O or Zr–Fe–O system do not react with the Zr–V and Zr–Fe melt, respectively, and, as a rule, can be identified as separate phases (e.g. Y_2O_3) on the XRD pattern (region I in Fig. 4). A weak interaction (manifested by the disappearance of the original oxide additive without formation of the η-phase; region II) was observed for Zr–V alloys at close values of the oxidation potentials of the oxide and Zr–V–O system, as well as for all Zr–Fe alloys when the oxidation potential of the oxide additive was below that of Zr–Fe–O. In the latter case, the formation of the η-phase took place after annealing [140]. Finally, Zr–V alloys with oxide additives characterised by higher oxidation potentials than Zr–V–O, exhibited the appearance of the η-phase in the as-cast state (shown by the strong interaction; region III).

In spite of the insignificant changes in the oxidation potentials of the oxides in Zr–V and Zr–Fe melts, the possibility of their interaction with the melt strongly depends on the nature of the alloying component (M) which significantly changes the oxidation potential of the Zr–M–O system. Comparing oxidation potentials of Ti–TiO ($-\lg(P_o) = 12.236$ at $T = 2030\ K$) and Zr–ZrO_2 ($-\lg(P_O) = 12.706$ at $T = 2000\ K$) [136], we can conclude that similar effects are expected for the titanium alloys, and the most stable ceramic materials suitable for the melting of Ti and its alloys would be Y_2O_3 and ZrO_2.

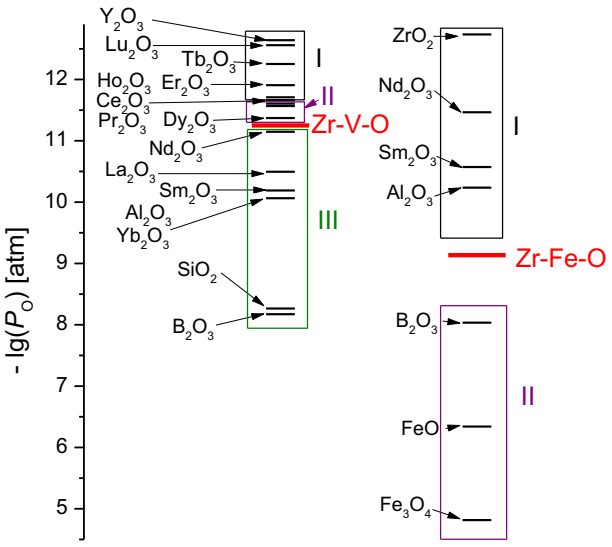

Fig. 4. Calculated oxidation potentials ($T = 2000$ K) of various oxides in Zr–V [139] and Zr–Fe [140] systems. Red lines correspond to the oxidation potential of Zr–V–O and Zr–Fe–O systems [136]. Rectangular regions correspond to the experimental observations: I – no interaction, II – weak interaction without formation of η-phase after solidification, III – strong interaction with formation of η-phase after solidification.

It should be noted that the thermodynamic approach disregards the solubility of metallic species or erosion in titanium melts so it should only be considered as the starting stage in crucible selection [112].

4.3. Shock resistance and other factors

Thermal shock resistance is a critical parameter in crucible selection and design for melting titanium alloys. This is due to large thermal gradients involved during processing when attempting to avoid long contact times between the crucible and molten titanium. The impact is more severe when dealing with large crucibles. For preliminary determination of crucible-melt interaction severity and wettability, sessile drop tests are performed on potential crucible materials using a typical set-up like the one shown in Fig. 5. One advantage of poor wettability between the ceramic crucible and molten titanium alloy will be a decrease in the degree of infiltration and erosion of the refractory by the melt [141]. After determining the candidate material, crucibles are manufactured by either slip casting or pressing of powders. For a particular crucible, the grain sizes and their distribution determines the final properties of the crucible, including porosity and shock resistance [45,46].

Data on melting, softening points, shock resistance, and Ellingham free energy of formation for selected potential refractory materials are compiled in Table 3. The crucible material should have higher melting and softening temperatures than superheated titanium (1668 °C) to be able to withstand and contain the molten metal. For example, SiO_2 (m.p. = 1710 °C) cannot properly withstand the temperatures involved in melting titanium and would result in aggressive contamination occurring due to softening at a temperature of 1280 °C. To obtain data for thermal shock resistance, thermal cycling tests are used to determine the number of cycles the crucible material can withstand before cracking, and the information can be converted to thermal shock resistance index values which are shown in Table 3. Generally, ceramic crucibles have low thermal shock resistance when compared to refractory metal crucibles, and this poses a challenge in upgrading ceramics crucibles. Highly thermal shock resistant crucibles are those which exhibit low thermal expansion coefficient and high thermal conductivity.

4.4. Crucible coating

It is difficult to find a crucible material which possesses both good thermal shock resistance and chemical inertness to a molten titanium alloy. Table 3 demonstrates that in traditional ceramic oxides, more shock resistant crucibles are generally less inert to molten titanium whilst more inert crucibles have poor thermal shock resistance. For example, although cheaper Al_2O_3 and MgO are less thermodynamically stable than ZrO_2, CaO and Y_2O_3, they demonstrate higher thermal shock resistance. Note that from Table 3, shock resistant materials are those with high thermal conductivities and low thermal expansion coefficients. Thermal shock resistance (R) parameter of refractories can be calculated using the following equation [146]:

$$R = \frac{\sigma(1-\upsilon)}{E\alpha} \tag{5}$$

where σ represents impact strength of the ceramic material, E is the elastic modulus, α is coefficient of thermal expansion, and υ is the Poisson's ratio.

The cost of ceramic materials generally increases with increasing thermodynamic stability. Therefore, the best practice would be to select a shock resistant crucible and then coat it with a thin inert material layer using either plasma spraying or slurry painting for protection from the reactive molten metal. For example, previous researchers have used an Al_2O_3 crucible coated with Y_2O_3 inert material [37,147] which results in good thermal shock resistance, low cost and chemical inertness to the molten titanium. In addition to inertness, the coating refractory material must be adherent and shock resistant to avoid cracking during thermal cycling, mechanically strong to resist solid feed abrasion when loading the crucible, and non-wettable to avoid erosion by the melt. Due to its high chemical inertness, Y_2O_3 has been widely studied as a coating material for induction melting crucibles [30,34,49,55,56,120–122,148]. To date, investigations on Y_2O_3 have been mainly focused on improving chemical inertness to avoid melt contamination and issues of thermal shock resistance have been rarely reported. The challenges in using Y_2O_3 coating is the poor shelf life of its slurry, poor sinterability, low adhesion to many substrates, and cracking due to thermal shock for thick

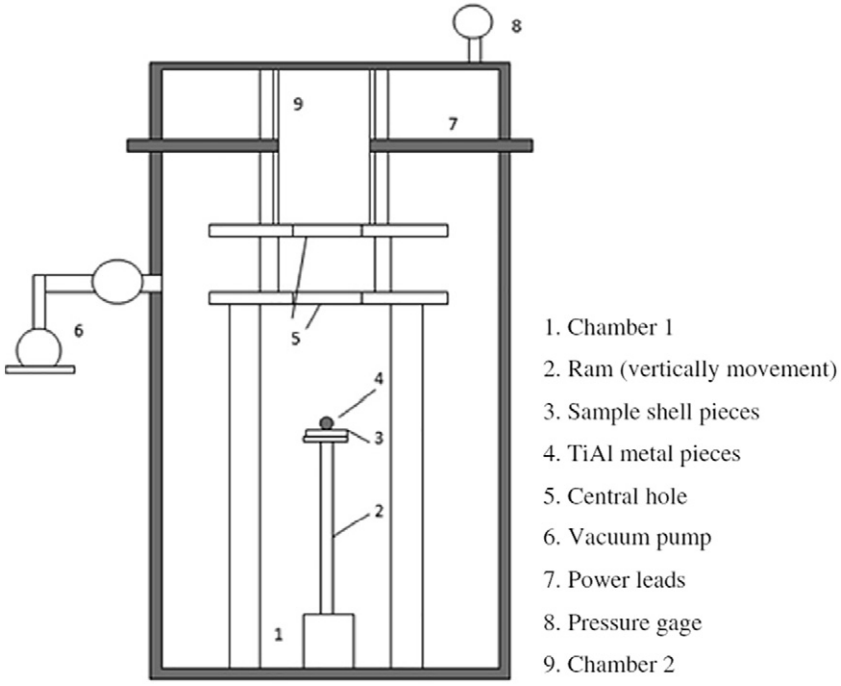

Fig. 5. The typical sessile drop "flash remelt" furnace structure with annotations [142–144].

Table 3
Prospective refractory materials for high temperature applications [71,145].

Refractory Material	Stability 2000K (-ΔG kJ/mol O_2)	Thermal Conductivity ($Wm^{-1}K^{-1}$)	Thermal Expansion Coefficient ($x10^{-6}K^{-1}$) 20–1000C	Melting (softening) Point/°C	Thermal shock resistance index	Cost
SiO_2	550.7	1.2–1.4	0.5–0.8	1710(1280)	93	Cheap
Al_2O_3	702.6	38	8.0	2072(1540)	19–26	Fair
MgO	660.0	30–60	9–12	2852(2100)	18	Fair
CaO	809.0	30	15.2	2572(1950)	–	Fair
ZrO_2	725.5	2.5	10.0	2715(2010)	12–13	Fair
Y_2O_3	891.3	8–12	8.1	2425(1855)	–	Expensive
AlN	–	280	4.5	2200(−)	37	Expensive
BeO	214	370	8	2507	–	Expensive
BN	–	1300	7.5	2200(−)	–	Expensive
Graphite	–	140	0.6–5.2	3530(2680)	–	Cheap

coatings. Several approaches to improve slurry life and sinterability were performed for Y_2O_3 coatings in investment casting moulds and these usually involve introducing low melting point additives, such as SiO_2 which lowers the inertness of the coating [34,148]. It should be noted that such additives cannot be used for Y_2O_3 coatings in melting crucibles due to the severity of melting reactions. An effective coating should be optimized in thickness to be capable of being used several times whilst being shock resistant to avoid thermal cracking. Research on crucible coating thickness optimisation for induction melting is scarce, and although there are several reports on the use of ~ 200–350 μm thick Y_2O_3 layers [56,122,148,149], there is no comprehensive research available in this area. In addition, work on the optimisation of thermal shock resistance and porosity of the coating is also still scarce.

We note that porosity is a very important parameter for both crucible body/substrate and the coating [33,45,46,49,150,151]. The increase of porosity results in a higher surface wettability and melt infiltration thus intensifying erosion processes during the melt and causing premature crack of the crucible or its coating when the infiltrated melt solidifies in the pores. Conversely, porosity improves shock resistance and facilitates adhesion of the coating to the substrate. Thus selection of an optimal porosity is a key issue for the crucible design.

Gomes et al. [56] used a centrifugal coating of an emulsion of Y_2O_3 slurry to produce a functionally graded 200 μm coating, with the particle size increasing from the inside of the crucible to the outside (close to the melt). The coating morphology was found to be good, to prevent crucible erosion, while at the same time maintaining high thermal shock resistance. Further research is still, however, necessary to establish the optimum coating thickness required for shock resistance whilst protecting the crucible from the aggressive melt for several melts. This may involve preparing Y_2O_3 slurries of different grain sizes and coating the crucible with different layers; e.g. sequential coating with a coarse to fine grain slurry (such as starting with a slurry of 30–60 μm grain size, a second slurry with 10–30 μm grain size and a third slurry with 1–5 μm grain size) to produce a dense and shock resistant functionally graded coating. Research has shown that so far AlN [27] is the only material identified which combines good shock resistance and chemical inertness to molten titanium and it can, subsequently, be directly used as a crucible material without the need for coating (Table 3). The main drawback to AlN is that it is expensive so can only be considered economical when applied as a thin layer coating to conventional crucibles. Table 3 shows that refractory materials based on AlN, BeO, BN and graphite demonstrate the best thermal shock resistance. When considering traditional ceramic oxides, Al_2O_3 and MgO are better for shock resistance. Note that refractory materials which are good as melting crucibles automatically perform better as investment casting moulds since melt-refractory reactions are less severe in casting compared to melting.

5. Crucibles for induction melting titanium alloys

As shown in Section 2, a possible way to reduce the production costs of Ti-based alloys could be the use of conventional ceramic crucibles for the induction melting process, utilising suitable and low cost ceramic materials for crucible production [76]. However, no suitable refractory material for crucible production of titanium based alloys has been identified so far. Melt-crucible interactions are always present to a certain extent, leading to alloy contamination and consequently chemical heterogeneity, as well as the development of solidification defects during castings. Specific crucible materials are necessary for each Ti-alloy since the aggressiveness of the melt depends on the alloy composition. Frueh et al. [25] performed a review of moulds for casting titanium alloys. Since crucibles experience more aggressive environments than moulds, the ability to develop melting crucibles will also solve the moulding materials challenge.

5.1. TiAl-based alloys

Over the last two decades, significant research aimed at the development of a suitable ceramic crucible to melt titanium – aluminium alloys has been carried out. The main undesirable impurities for these alloys are oxygen and carbon and, according to many industrial standards, the oxygen content should not exceed 0.1 wt% [36]. A summary of the performances of different crucible materials used to melt TiAl alloys is shown in Table 1. The table shows that much research has been performed on crucible materials for induction melting of γ-TiAl alloys and this is due to their attractive properties, coupled with less aggressiveness of the melt. In addition, Table 1 also highlights that ceramic oxides, ceramic non-oxides and refractory metals are potential crucibles for melting titanium alloys; these will be discussed in more detail in the next sections.

5.1.1. Ceramic oxide crucibles

Several different oxides, carbides, borides and sulphides have been evaluated for melting titanium alloys but, in general, the results reported have been unsatisfactory due to chemical incompatibility with the cast alloys and/or poor thermal-shock resistance of the crucibles, leading to crack development and crucible destruction [25]. As a result, repeated melts cannot be prepared in the same crucible because of failure during melting or cooling. Among the tested materials, ceramic oxides, in particular CaO [76,115] and Y_2O_3 [42,55,113,122] were found to perform best in chemical inertness. Although Y_2O_3 and CaO are more thermodynamically stable than TiO, they are both poor in shock resistance. In addition, CaO is hygroscopic while Y_2O_3 is expensive and both crucible materials are prone to slight reactions with titanium alloys. Such reactions result in an undesirable increase in oxygen content in the produced castings and, as such, their use is currently restricted to non-critical applications. Many small ceramic oxide crucibles have been tested at laboratory scale. However, more often than not, these crucibles are usually only used once due to cracking caused by thermal shock. Ceramic oxide crucibles are generally manufactured with some level of porosity to improve their shock resistance but this makes them susceptible to melt infiltration and erosion attack. There has been work reported on the use of cheap and better shock resistant crucibles which are coated

with inert materials to combine thermal shock resistance with chemical inertness. For example, Y_2O_3 showed the best performance with molten TiAl, with an interaction layer thickness of <20 μm and low oxygen contamination in ingots. Table 1 shows that aside from Y_2O_3, no other ceramic oxide meets the minimum requirements of <0.1 wt% oxygen in ingots. The best ceramic oxide crucibles are those which exhibit high shock resistance, e.g. Al_2O_3 coated with a layer of inert material like Y_2O_3, and an example of such a crucible was applied during a Bridgeman directional solidification process performed by Zhang et al. [37,116].

A typical ZrO_2 crucible, in which the interior is brush coated with a slurry of pure Y_2O_3 to enhance the chemical inertness, is shown in Fig. 6. A reaction product layer, like the one shown in Fig. 7, develops during the melting and solidification of an alloy inside the crucible due to crucible melt interactions, and will be thin when using the inert protection material. Some of the research compiled in Table 1 shows that Y_2O_3 is the only ceramic oxide capable of melting more aggressive alloys like Ti6AlV with slight contamination, while lesser aggressive alloys such as γ-TiAl can be satisfactorily melted in CaO crucibles [47]. Other promising ceramic oxides with good thermal shock resistance and chemical inertness, like beryllium oxide (BeO), have yet to be fully investigated. BeO is the only known ceramic oxide with high thermal conductivity and a small thermal expansion coefficient, which results in good overall thermal shock resistance. Thus, a dense BeO crucible with closed pores is both erosion and shock resistant and is worthy investigating. It may be necessary to study the use of thermal shock resistant and chemically inert refractory materials like AlN [30] for coating shock resistant ceramic oxide crucibles like Al_2O_3 or MgO.

In addition to these ceramic oxides, composite ceramic oxides were demonstrated to be of high thermal stability as crucible materials for melting titanium alloys. $CaZrO_3$ and $BaZrO_3$ composites have been shown to be potential refractories for melting titanium alloys. $CaZrO_3$ was used as the mould material for Ti alloys and showed low corrosion properties similar to CaO [43]. The interactions between $CaZrO_3$ crucibles and Ti6Al4V/TiAl alloys were investigated by Schaffoner [57,152] and were demonstrated to be of good corrosion resistance against Ti melts. Li et al. [123] developed a $CaZrO_3$ crucible by sintering ZrO_2 and CaO powders. In this study, an interaction layer thickness of approximately 350 μm was detected at the Ti6Al4V (Ti64) alloy surface, with some oxides present. In comparison to $CaZrO_3$, research on $BaZrO_3$ [127,153] showed that no apparent interaction layer was observed and the oxygen contamination was lower than in Y_2O_3 crucibles. The application of a $BaZrO_3$ shell mould for the directional solidification of TiAl alloys was studied by He et al. [155]. Li et al. [154] prepared a TiFe alloy using a $BaZrO_3$ crucible and found that the end alloy achieved better hydrogen storage properties in comparison to an alloy produced using a graphite crucible. Improved stability for the $BaZrO_3$ was achieved after doping with CaO [128] and $CaZrO_3$ was improved after adding Al_2O_3 [125]. This was attributed to low wetting behaviour of these ceramic crucibles. $CaZrO_3$ doped with Al_2O_3, Y_2O_3 and MgO have been shown to possess high chemical stability and very good tolerance against thermal shock [156].

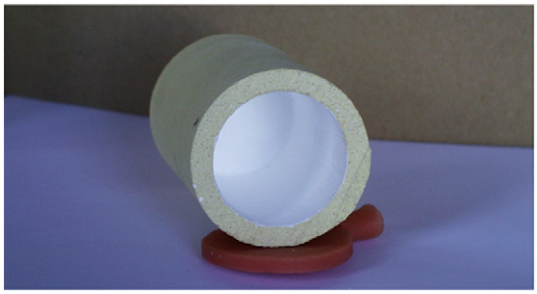

Fig. 6. ZrO_2 crucible inside coated with Y_2O_3 [120].

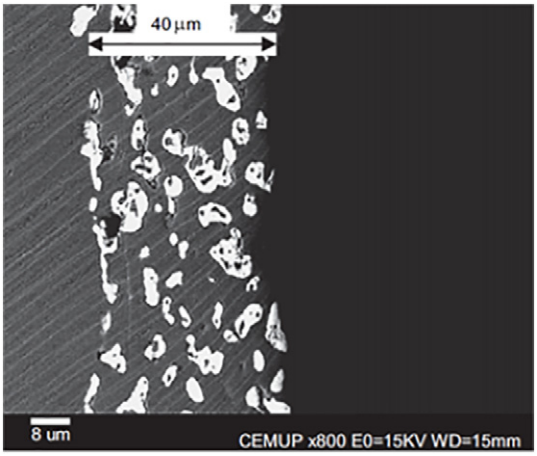

Fig. 7. Y_2O_3 layer at the cast Ti-48Al samples surface for holding time of 90 s at 1600 °C using Y_2O_3 crucible [55].

Chinese patents [157,158] have shown that both $CaZrO_3$ and $BaZrO_3$ crucibles can be used for melting Ti-containing alloys. The crucibles remain undamaged and clean while no crucible material was found on the surface of the as-prepared alloys. The large scale production of these crucibles is still, however, a significant challenge due to the complexity of the production process, coupled with high costs.

Routes for the preparation of $BaZrO_3$ ceramics via a solid state reaction of $BaCO_3$ with ZrO_2 (followed by cold isostatic pressing or sintering of the crucible) have recently been developed [159]. Further modifications of the method include doping of the ceramics with CaO [160,161] or Y_2O_3 [162,163]. The latter was shown to be particularly promising for making crucibles for melting TiNi alloys; no obvious interaction layer and element diffusion between the crucible and the melt were observed [163]. Y_2O_3 doped $BaZrO_3$ was also successfully applied as a coating for Al_2O_3 crucibles used for investment casting of titanium alloy [164].

5.1.2. Non-oxide crucibles

Unlike ceramic oxides, non-oxide materials avoid contamination of the molten metal by oxygen. Amongst the non-oxide refractories, nitrides and refractory metals possess promising properties for melting titanium alloys. Note that only a few ceramics possess high thermal conductivity and these are Beryllium Oxide (BeO), Boron Nitride (c-BN) and AlN.

5.1.2.1. Nitrides. To minimize oxygen contamination of the melt, non-oxide materials like AlN and BN have been evaluated for melting TiAl alloys [30]. BN showed poor performance; causing aggressive melt contamination in addition to being expensive and difficult to produce. On the other hand, AlN is a unique ceramic material, which combines high thermal conductivity with high electrical resistivity. AlN has been found to perform quite well with a small interaction layer thickness, leading to non-contaminated castings with good ingot release after solidifying inside the crucible [30]. High density AlN crucibles combine chemical inertness with good shock and erosion resistance. However, they are expensive and large crucible fabrication is difficult. As a result of this, AlN can only be economically used as thin coatings on shock resistant crucibles like Al_2O_3 or graphite. From a coating perspective, slurry based coating methods like air spraying or painting cannot be used due to the high reactivity of AlN with water so, in general, techniques like plasma coating are used.

5.1.2.2. Graphite and refractory metals. Graphite (C) and refractory metals like molybdenum (Mo), niobium (Nb), tungsten (W) and tantalum (Ta) have the potential for use as crucible materials because of their good shock resistance and high melting and softening temperatures.

However, the direct application of graphite and pure refractory metal crucibles has been shown to suffer from attack from the melts due to high chemical reactivity (thermodynamic instability) and dissolution [165]. Graphite has been shown to perform better than several of the examined oxides, carbides, nitrides, silicides, and refractory metals (Mo and W) in reacting to titanium alloys [166–169]. For practical use, refractory metal crucibles should be protected with thermodynamically stable materials such as Y_2O_3 [166–171]. The main challenge to overcome when graphite is coated is carbon diffusion. This leads to the coating being degraded, due to saturation with carbides, and over time the melt can become severely contaminated. It has been shown that single layers of non-oxides, carbides and oxides on graphite failed to completely prevent carbon diffusion into the melt, particularly for high temperature melting [1]. The use of multilayer coatings was found to prevent carbon diffusion for a number of melts. However, once the layers became saturated with carbon, excessive melt contamination occurred [5]. Multilayer coatings of refractory metals and ceramic oxides on graphite have been proposed but the issue remains that melting titanium will lead to transformation of the refractory metal to a carbide, which will continuously reduce the effective thickness of the coating [168]. It was shown that coating graphite with refractory and carbide forming metals, like Mo, W and Nb, before applying a final coating of inert refractories like Y_2O_3 proved good for preventing carbon diffusion into the melt for a significant number of melts [168]. In spite of this, TiAl alloys have still not been effectively melted in graphite crucibles due to contamination levels above the required industrial standards. The graphite coating technology has, however, been successfully applied for the melting of uranium alloys [168,169]. More research is needed in coating refractory metal crucibles like Mo, W and Ta with inert materials like Y_2O_3 or AlN for induction melting titanium alloys. Such refractory metals have lower diffusion rates than carbon at high temperatures, so once coated they will not contaminate the melt. Table 1 shows that TiAl alloys melted in graphite crucibles exhibit a high carbon content, due to aggressive carbon diffusion into the melt at high processing temperatures so, in most cases, they fail to meet the required industrial standards.

5.2. NiTi alloys

The ideal crucible for melting NiTi alloys should possess good thermal shock resistance, be low in cost, inert to the molten NiTi alloy and, most importantly, should not release oxygen into the melt. Oxygen contamination in the melt occurs either from the input raw materials or from the furnace atmosphere. The furnace should, therefore, be properly sealed and raw materials should be of high purity (i.e. ≥99.9%). Even commercial, high grade Ti may contain too much oxygen for acceptable shape memory properties. Thus, by virtue of releasing oxygen into the melt, ceramic oxide crucibles, such as CaO, ZrO_2, Y_2O_3, MgO, and Al_2O_3, are not suitable for use in VIM processing NiTi based alloys [32]. Instead, VIM with non-oxide, high density graphite crucibles is currently used to minimize carbon contamination of the melt [40,44,130].

The advantages of graphite crucibles include; easy handling, low price, minimal erosion and high thermal shock resistance and the ability to produce highly homogenous alloys [40,44,130]. However, the undesirable reaction between a NiTi melt and a graphite crucible is inevitable; forming carbides which affect the final alloy composition and purity [131]. The carbon content in the melt increases with increasing both the melting temperature and interaction time (Fig. 8). During the first contact of the NiTi melt with the crucible, a protective TiC layer is formed on the inner surface of the crucible (similar to the one shown in Fig. 9), which advantageously acts as a diffusion barrier for the subsequent castings. The arrangement of the charge in the crucible is also very important in VIM of NiTi alloys [44,131]. A significant reduction in carbon content can be achieved by avoiding the direct contact between Ni and graphite and this can be achieved through Ti-disk cladding, which quickly forms a TiC protective layer on the crucible surface [131]. According to several industrial standards, e.g. the American Society for Testing and Materials (ASTM), the maximum acceptable oxygen and carbon content of NiTi alloys should not exceed 0.05 wt% [40]. Table 2 shows the crucible-melt interaction parameters for NiTi based SMA's produced using different crucibles. Besides graphite, Table 2 shows that ceramic oxide materials fail to meet quality standards. Future work on crucibles for melting NiTi alloys should, therefore, focus on further improving the quality of the final alloy through reduction of the contamination level. Other non-oxide refractory alternatives with high shock resistance, like BN and AlN, should also be investigated as either crucible materials or as coatings to refractory crucibles.

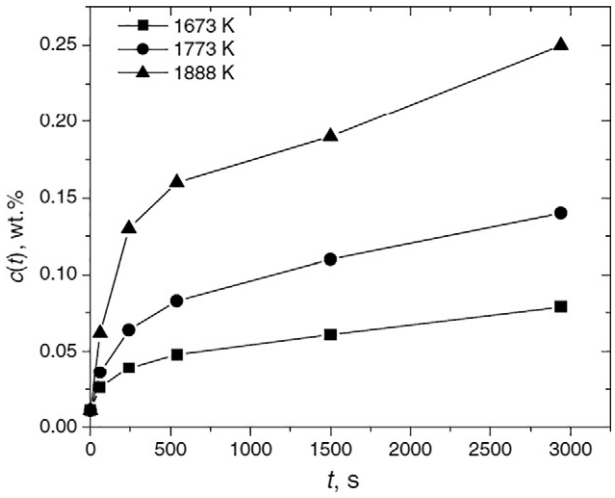

Fig. 8. Results of the chemical analysis showing the increase of carbon content in NiTi melts at 1673(1400 °C), 1773(1500 °C) and 1888 K(1615 °C) after different reaction times [131].

5.3. Hydrogen storage alloys

As mentioned in Section 3.3, hydrogen storage alloys are very sensitive to contamination by non-metallic impurities, deviations from target composition and inhomogeneities. The identification and selection of suitable crucible materials is a challenging task; conventional crucibles based on SiO_2, Al_2O_3 or carbon are excluded from direct use. In addition, optimisation of the lining and/or coating material requires comprehensive and time-consuming experimental studies [11].

Only a few studies on crucible materials for melting Ti-based hydrogen storage alloys were identified in the literature. The melting of TiFe in a graphite crucible [172] was shown to result in contamination of the ingot by carbon, which led to a significant reduction in the hydrogen sorption performance. Further, the interaction of the melt with graphite was found to form TiC, which strongly sticks to the crucible wall (Fig. 10A). More dramatic changes take place when attempting to

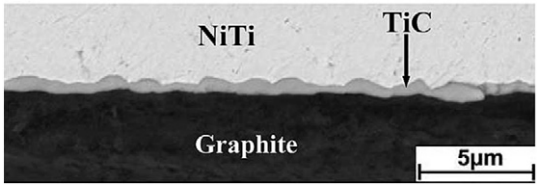

Fig. 9. SEM micrographs showing the interface region between the graphite crucible and a NiTi alloy [131].

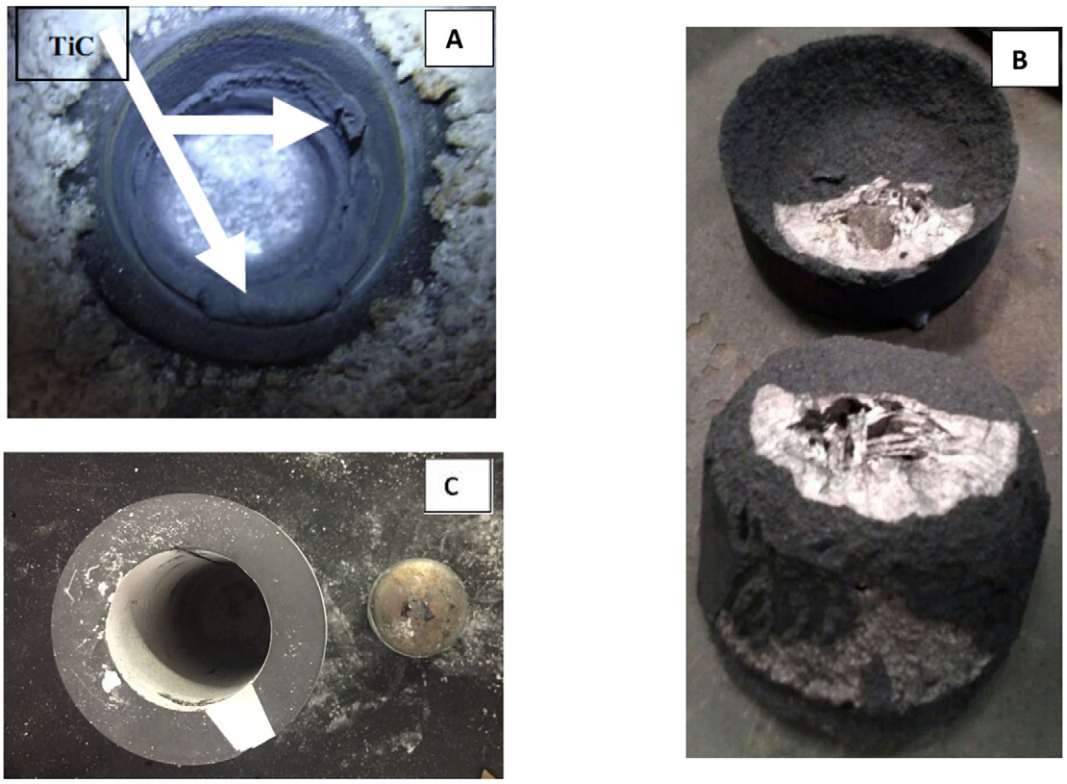

Fig. 10. Images of graphite crucibles after melting Ti alloys at T~1600 °C. A – $TiFe_{0.86}Mn_{0.1}$ [172]; B, C – $Ti_{0.85}Zr_{0.15}Mn_{1.2}M_{0.8}$ AB_2-type alloy (M = V + Cr + Ni + Fe; our data). The crucible shown in C was lined with multi-layer coating with Y_2O_3 as a melt-facing layer.

melt Ti and Zr based AB_2-type alloy containing large amounts of Mn which is known to form carbides below 1300 °C [72]; vol.1, pp.859–861. Severe interaction of the melt with the graphite resulted in complete disintegration of the crucible and strong adhesion of the melt to the crucible (Fig. 10B).

Based on the literature, it was recommended to use crucibles made of CaO [172], $BaZrO_3$ [154] or $CaZrO_3$ [173] for melting TiFe-based alloys. The first solution seems to be problematic in the large-scale manufacturing due to high affinity of CaO to water vapours and CO_2 in the atmosphere. The resistance of CaO refractories towards interacting with water vapours can, however, be significantly increased by doping with Y_2O_3, which results in the formation of metastable CaY_2O_4 phase on grain boundaries [174].

Due to similar melting conditions and, accordingly, similar requirements to the crucible materials for manufacturing TiAl and Ti-based hydrogen storage alloys, it is expected that the selection criteria for crucibles necessary for induction melting the latter product will be similar. However, the features required in the preparation of hydrogen storage alloys (e.g. the necessity to add zirconium or rare-earth metal deoxidizers which increase the chemical aggressiveness of the melt) pose additional challenges to crucible design, which also need to be taken into account in future studies. Solutions related to lining the crucibles with high thermal shock resistance chemically inert coatings (see section 4.4) seem to be particularly promising.

Recent experimental studies carried out by the authors have shown a satisfactory performance of crucibles made of Al_2O_3, $Al_2O_3{\cdot}SiO_2$ and low-density graphite lined with multilayer coatings where the external (facing the melt) layer used was Y_2O_3. Trial melts of an AB_2-type alloy (see example in Fig. 10C) did not stick to the crucible even after solidification inside, and the differences in hydrogen sorption properties of the alloys in comparison to a reference sample produced by arc-melting were insignificant. The results of these experimental studies will be published in a due course.

6. Conclusions and perspectives

Amongst a wide range of techniques for melting titanium alloys for various applications, vacuum induction melting is very promising due to its simplicity, flexibility and the ability to produce homogeneous ingots. However, the main challenge for this method is the difficulty of selection of suitable crucibles, which must be tolerant towards interaction with aggressive melt at high temperature, as well as resistant to thermal shock.

This review showed that significant progress has been made in designing crucibles for melting titanium alloys with minimum crucible – melt interactions. However, there are still technological issues which limit the use of the newly-developed crucibles in large scale induction melting of titanium alloys. The major challenge is the unavailability of crucibles which combine the following features:

(i) Low contamination of the ingot;
(ii) Long service lifetime;
(iii) High tolerance towards attack with the aggressive titanium-containing melt;
(iv) Stability at high temperatures (≥1600 °C);
(v) High thermal shock resistance;
(vi) Low wettability under melting conditions.

Experiments guided by thermodynamic studies have demonstrated that vacuum induction melting of Ti alloys in refractory oxide or non-oxide crucibles is generally possible but further research is needed to meet the required purity of the final product. The contamination levels of the alloys prepared by induction melting should be comparable to the ones for industrial-scale crucible-free melting methods.

Amongst the studied crucible materials, Y_2O_3, $CaZrO_3$- Al_2O_3 composite, $BaZrO_3$, CaO- and Y_2O_3-doped $BaZrO_3$, and AlN were shown to be able to produce alloys which, in most cases, meet the required

industrial standards of low oxygen content (<0.1 wt%) and thin interaction layers. Work is still needed to upgrade these crucibles from laboratory to industrial scale taking into account material cost, thermal shock failure and contamination of the ingot. The focus of future developments in this area should, therefore, be put on crucible material and design solutions, which address these contradictory problems simultaneously. Coating of inexpensive and shock-resistant but insufficiently inert crucibles (e.g. Al_2O_3 or graphite) with materials chemically stable to the interaction with the melt at the high temperatures (e.g. Y_2O_3) seems to be a promising solution. However, there are still several issues relating to the stability of the coating and providing good adhesion to the crucible body, which need to be overcome. Special attention should be paid to upscaling coating technology; including ease of recoating after melting and slurry stability.

Other promising systems like AlN non-oxide refractory crucibles, exhibit excellent thermal shock resistance and low reactivity with titanium melt but have, to date, only been studied at laboratory scale so further research for the upscaling are necessary. Detailed studies combining parameters including; reactivity, thermal shock, manufacturability and cost-benefit analysis are in a great demand.

The results from this review indicate that promising crucibles with potential for upscaling to melt various titanium containing alloys are the following:

a. Inexpensive and shock resistant crucibles characterised by high melting or softening temperatures (e.g. Al_2O_3 or graphite) coated inside with thin inert refractory materials (e.g. Y_2O_3);
b. Shock resistant AlN crucibles;
c. Shock resistant refractory metals (e.g. Ta, W, Mo) coated with inert materials (e.g. Y_2O_3);
d. Ceramic composites like $BaZrO_3$ and CaO-doped $BaZrO_3$ crucibles.

CRediT authorship contribution statement

Simbarashe Fashu: Formal analysis, Writing - original draft. **Mykhaylo Lototskyy:** Conceptualization, Project administration, Supervision, Writing - review & editing. **Moegamat Wafeeq Davids:** Data curation, Funding acquisition, Investigation. **Lydia Pickering:** Investigation, Validation, Writing - review & editing. **Vladimir Linkov:** Project administration, Resources. **Sun Tai:** Data curation, Validation. **Tang Renheng:** Conceptualization, Supervision. **Xiao Fangming:** Project administration. **Pavel V. Fursikov:** Formal analysis. **Boris P. Tarasov:** Formal analysis.

Acknowledgements

All the authors acknowledge support of BRICS STI Framework Programme (project 064 - RICS-MH). The work of South African team was funded by the Department of Science and Technology (DST) of South Africa within Hydrogen South Africa (HySA) Programme; projects KP3-S02, KP6-S01, KP8-S05 and special innovation project "South African Metal Hydride Alloys: Proof of Concept". ML and MWD also acknowledge support of the National Research Foundation of South Africa (Grant Numbers 109092 and 116278, respectively). The Chinese co-authors got co-finding from MOST Scientific Project (YS2018YFGH000067) and Guangdong Scientific Projects (No. 2017B030314081, No. 2017GDASCX-0506, 2019GDASYL-0503005). The Russian co-authors are grateful for the financial support of the Ministry of Science and Higher Education of Russian Federation, Agreement No. 14.613.21.0087, Unique Identifier RFMEFI61318X0087.

Appendix A. Supplementary data

Supplementary data to this article can be found online at https://doi.org/10.1016/j.matdes.2019.108295.

References

[1] C. Leyens, M. Peters (Eds.), Titanium and Titanium Alloys: Fundamentals and Applications, Wiley-VCH, Weinheim 2003, p. 513.
[2] W. Sha, S. Malinov, Titanium Alloys. Modelling of Microstructure, Properties and Applications, Woodhead Publ, 2009 569.
[3] C. Veiga, J.P. Davim, A.J.R. Loureiro, Properties and applications of titanium alloys: a brief review, Rev. Adv. Mater. Sci. 32 (2012) 133–148.
[4] F.H. Froes, H. Friedrich, J. Kiese, D. Bergoint, Titanium in the family automobile: the cost challenge, J. Miner. Met. Mater. Soc. 56 (2) (2004) 40–44, https://doi.org/10.1007/s11837-004-0144-0.
[5] F.H.S. Froes, M.N. Gungor, M.A. Imam, Cost-affordable titanium: the component fabrication perspective, J. Miner. Met. Mater. Soc. 59 (6) (2007) 28–31, https://doi.org/10.1007/s11837-007-0074-8.
[6] R.R. Boyer, Titanium for aerospace: rationale and applications, Adv. Perform. Mater. 2 (4) (1995) 349–368.
[7] I.V. Gorynin, Titanium alloys for marine application, Mater. Sci. Eng. A 263 (2) (1999) 112–116.
[8] H.J. Rack, J.I. Qazi, Titanium alloys for biomedical applications, Mater. Sci. Eng. C 26 (8) (2006) 1269–1277.
[9] Z. Yu, G. Wang, X. Ma, Y. Zhang, M.S. Dargusch, Shape memory characteristics of a near β titanium alloy, Mater. Sci. Eng. A 513–514 (2009) 233–238.
[10] A.N. Khan, M. Muhyuddin, A. Wadood, Development and characterization of nickel–titanium–zirconium shape memory alloy for engineering applications, Russ. J. Non-Ferrous Metals 58 (5) (2017) 509–515.
[11] B. Friedrich, Large-scale production and quality assurance of hydrogen storage (battery) alloys, J. Mater. Eng. Perform. 3 (1) (1994) 37–46.
[12] A. Martínez, D.S. dos Santos, Hydrogen absorption/desorption properties in the TiCrV based alloys, Mater. Res. 15 (5) (2012) 809–812.
[13] L. Pickering, D. Reed, A.I. Bevan, D. Book, Ti–V–Mn based metal hydrides for hydrogen compression applications, J. Alloy. Comp. 645 (2015) S400–S403.
[14] L. Pickering, M.V. Lototskyy, M.W. Davids, C. Sita, V. Linkov, Induction melted AB_2-type metal hydrides for hydrogen storage and compression applications, Mater. Today: SAVE Proc. 5 (2018) 10470–10478.
[15] An Overview of South Africa's Titanium Mineral Concentrate Industry, Department of mineral resources: Republic of South Africa, Directorate: Mineral Economics, Report R71/2008. http://www.dmr.gov.za.
[16] reportOverview of South Africa's Titanium Industry and Global Market Review, 2012, Department of mineral resources: Republic of South Africa, Directorate: Mineral Economics, Report R104/2013. http://www.dmr.gov.za.
[17] S.A.C. Hockaday, K. Bisaka, Experience and results from running of a 1 kg Ti scale kroll reactor, The Southern African Institute of Mining and Metallurgy Advanced Metals Initiative, Light Metals Conference 2010, pp. 265–280. https://www.pyrometallurgy.co.za/Mintek/Files/2010Hockaday2.pdf.
[18] L. Van Der Merwe, G. Ruthven, K. Von Leipzig, The study and design of a national supply chain for the aerospace titanium components manufacturing industry, J. Trans. Suppl. Chain Manag. (2012) 15–34.
[19] M. Dworzanowski, The role of metallurgy in enhancing beneficiation in the South African mining industry, J. S. Afr. Inst. Min. Metall 113 (2013) 677–683.
[20] U.S. Geological Survey, Mineral commodity summaries, https://minerals.usgs.gov/minerals/pubs/commodity/.
[21] TITANIUM USA 2018Oct. 7-10, 2018, Las Vegas, USA. Executive Summary https://cdn.ymaws.com/titanium.org/resource/resmgr/02_jens_folder/titanium_usa_2018_executive_.pdf.
[22] China's Titanium Production Rises in 2018. , Argus Media group, 2019, 26 April 2019 https://www.argusmedia.com/en/news/1891732-chinas-titanium-production-rises-in-2018.
[23] E.M. Savitskii, G.S. Burkhanov, Melting and treatment of refractory metals and alloys, Physical Metallurgy of Refractory Metals and Alloys, Springer 1970, pp. 235–283, https://doi.org/10.1007/978-1-4684-1572-8_7.
[24] B.C. Weber, W.M. Thompson, H.O. Bielstein, M.A. Schwartz, Ceramic crucible for melting titanium, J. Am. Chem. Soc. 40 (11) (1957) 363–373.
[25] R. Frueh, C. Poirier, D.R. Maguire, M.C. Harding, Attempts to develop a ceramic mould for titanium casting–a review, Int. J. Cast Met. Res. 9 (4) (1996) 233–239.
[26] C. Frueh, D.R. Poirier, M.C. Maguire, The effect of silica-containing binders on the titanium/face coat reaction, Metal. Mater. Trans. 28B (1997) 919–926.
[27] E.J. Chapin, H.W. Friske, A Metallurgical Evaluation of Refractory Compounds for Containing Molten Titanium. Part II - Carbon, Graphite, and Carbides, NRL Report 4487 Naval Research Laboratory, 1954. https://pdfs.semanticscholar.org/101e/a4e29c3520b7cc155b34931ceb9f90969d7c.pdf.
[28] G.V. Samsonov, G.A. Yasinskaya, T.S. Wei, High-melting carbide, boride and nitride crucibles, Refract. Ind. Ceram. 1 (1960) 26–29, https://doi.org/10.1007/BF01602875.
[29] A.W. Weimer (Ed.), Carbide, Nitride and Boride Materials Synthesis and Processing, Chapman & Hall 1997, p. 670.
[30] A.V. Kartavykh, V.V. Tcherdyntsev, J. Zollinger, TiAl-Nb melt interaction with AlN refractory crucibles, Mater. Chem. Phys. 116 (2009) 300–304.
[31] A.V. Kartavykh, V.V. Tcherdyntsev, J. Zollinger, TiAl–Nb melt interaction with pyrolytic boron nitride crucibles, Mater. Chem. Phys. 119 (2010) 347–350.
[32] S.K. Sadrnezhaad, S.B. Raz, Interaction between refractory crucible materials and the melted NiTi shape-memory alloy, Metall. Mater. Trans. B Process Metall. Mater. Process. Sci. 36 (3) (2005) 395–403, https://doi.org/10.1007/s11663-005-0068-2.
[33] E.D. Eastman, L. Brewer, L.A. Bromley, P.W. Gilles, N.I. Lofgren, Preparation and tests of refractory sulfide crucibles, J. Am. Ceram. Soc. 34 (4) (1951) 128–134.
[34] J.P. Kuang, R.A. Harding, J. Campbell, Investigation into refractories as crucible and mould materials for melting and casting γ -TiAl alloys, Mater. Sci. Technol. 16 (9) (2000) 1007–1016.

[35] K. Sakamoto, K. Yoshikawa, T. Kusamichi, T. Onoye, Changes in oxygen contents of titanium aluminides by vacuum induction, cold crucible induction and electron beam melting, ISIJ Int. 32 (5) (1992) 616–624.

[36] T. Tetsui, T. Kobayashi, T. Ueno, H. Harada, Consideration of the influence of contamination from oxide crucibles on TiAl cast material, and the possibility of achieving low-purity TiAl precision cast turbine wheels, Intermetallics 31 (2012) 274–281.

[37] H.R. Zhang, X.X. Tang, L. Zhou, M. Gao, C.G. Zhou, H. Zhang, Interactions between Ni-44Ti-5Al-2Nb-Mo alloy and oxide ceramics during directional solidification process, J. Mater. Sci. 47 (17) (2012) 6451–6458.

[38] Z. Zhang, J. Frenzel, K. Neuking, G. Eggeler, Vacuum induction melting of ternary NiTiX (X = Cu, Fe, Hf, Zr) shape memory alloys using graphite crucibles, Mater. Trans. 47 (3) (2006) 661–669.

[39] J. Frenzel, Z. Zhang, K. Neuking, G. Eggeler, High quality vacuum induction melting of small quantities of NiTi shape memory alloys in graphite crucibles, J. Alloy. Comp. 385 (1–2) (2004) 214–223.

[40] N. Nayan, Govind, C.N. Saikrishna, K.V. Ramaiah, S.K. Bhaumik, K.S. Nair, M.C. Mittal, Vacuum induction melting of NiTi shape memory alloys in graphite crucible, Mater. Sci. Eng. A 465 (1–2) (2007) 44–48.

[41] J. Kuang, J.P. Harding, R.A. Campbell, A study of refractories as crucible and mould materials for melting and casting γ-TiAl alloys, Int. J. Cast Met. Res. 13 (5) (2001) 277–292.

[42] L. Aihui, L. Bangsheng, N. Hai, S. Yanwei, G. Jingjie, F. Hengzhi, Study of interfacial reaction between TiAl alloys and four ceramic molds, Rare Metal Mater. Eng. 37 (6) (2008) 956–959, https://doi.org/10.1016/S1875-5372(09)60028-X.

[43] S.K. Kim, K. Kim, T.W. Hong, Y.J. Kim, Investment casting of titanium alloy with CaO crucible and $CaZrO_3$ mold, in: K. Jata, E.W. Lee, W. Frazier, N.J. Kim (Eds.),Lightweight Alloys for Aerospace Application TMS (The Minerals, Metals & Materials Society) 2001, pp. 251–260.

[44] J. Frenzel, K. Neuking, G. Eggeler, M. Werkstoff, Induction melting of NiTi shape memory alloys -The influence of the commercial crucible graphite on alloy quality, Mater. Sci. Eng. Technol. 35 (5) (2004) 352–358.

[45] T. Tetsui, T. Kobayashi, T. Mori, T. Kishimoto, H. Harada, Evaluation of yttria applicability as a crucible for induction melting of TiAl alloy, Mater. Trans. 51 (9) (2010) 1656–1662.

[46] T. Tetsui, T. Kobayashi, A. Kishimoto, H. Harada, Structural optimization of an yttria crucible for melting TiAl alloy, Intermetallics 20 (1) (2012) 16–23.

[47] C. Lochbichler, B. Friedrich, Direct deoxidisation of Ti and TiAl scrap recycling of Ti and TiAl alloys, in Proc. EMC 2007, June 26-29, Düsseldorf, Germany (GDMB), Clausthal-Zellerfeld, 2007, vol. vol. 1, (2007), p.81-88.

[48] J.J. Barbosa, C.S. Ribeiro, Influence of crucible material on the level of contamination in TiAl using induction melting, Int. J. Cast Met. Res 12 (5) (2000) 293–301.

[49] F. Gomes, J. Barbosa, C.S. Ribeiro, Evaluation of functionally graded ceramic crucible for induction melting of TiAl based alloys, Mater. Sci. Forum 730–732 (2013) 769–774.

[50] R.A. Harding, Recent developments in the induction skull melting and investment casting of titanium aluminides, Kov. Mater. 42 (4) (2004) 225–241.

[51] T. Tetsui, K. Shindo, S. Kaji, S. Kobayashi, M. Takeyama, Fabrication of TiAl components by means of hot forging and machining, Intermetallics 13 (9) (2005) 971–978.

[52] Z.Z. Fang, J.D. Paramore, P. Sun, K.S. Ravi Chandran, Y. Zhang, Y. Xia, F. Cao, M. Koopman, M. Free, Powder metallurgy of titanium – past, present, and future, Int. Mater. Rev. 63 (7) (2017) 407–459.

[53] X. Wu, Review of alloy and process development of TiAl alloys, Intermetallics 14 (10–11) (2006) 1114–1122.

[54] R.A. Harding, M. Wickins, H. Wang, G. Djambazov, K.A. Pericleous, Development of a turbulence-free casting technique for titanium aluminides, Intermetallics 19 (6) (2011) 805–813.

[55] J. Barbosa, C.S. Ribeiro, A.C. Monteiro, Influence of superheating on casting of γ-TiAl, Intermetallics 15 (7) (2007) 945–955.

[56] F. Gomes, H. Puga, J. Barbosa, C.S. Ribeiro, Effect of melting pressure and superheating on chemical composition and contamination of yttria-coated ceramic crucible induction melted titanium alloys, J. Mater. Sci. 46 (14) (2011) 4922–4936.

[57] S. Schafföner, C.G. Aneziris, H. Berek, J. Hubálková, B. Rotmann, B. Friedrich, Corrosion behavior of calcium zirconate refractories in contact with titanium aluminide melts, J. Eur. Ceram. Soc. 35 (3) (2015) 1097–1106.

[58] B. Rotmann, C. Lochbichler, B. Friedrich, Challenges in titanium recycling - do we need a new specification for secondary alloys? Proc. EMC 2011, June 26-29, Düsseldorf, Germany (GDMB), Clausthal-Zellerfeld, vol. 4, 2011, pp. 1465–1480.

[59] J.A. Van Den Avyle, J.A. Brooks, A.C. Powell, Reducing defects in remelting processes for high-performance alloys, J. Miner. Met. Mater. Soc. 50 (3) (1998) 22–25, https://doi.org/10.1007/s11837-998-0374-7.

[60] Y. Kabiri, A. Kermanpur, A. Foroozmehr, Comparative study on microstructure and homogeneity of NiTi shape memory alloy produced by copper boat induction melting and conventional vacuum arc melting, Vacuum 86 (8) (2012) 1073–1077.

[61] D.J. Chronister, S.W. Scott, D.R. Stickle, D. Eylon, F.H. Froes, Induction skull melting of titanium and other reactive alloys, J. Miner. Met. Mater. Soc. 38 (9) (1986) 51–54, https://doi.org/10.1007/BF03258690.

[62] M. Kazemipour, H. Salimijazi, A. Saidi, A. Saatchi, A. Aref Arjmand, Hydrogen storage properties of $Ti_{0.72}Zr_{0.28}Mn_{1.6}V_{0.4}$ alloy prepared by mechanical alloying and copper boat induction melting, Int. J. Hydrogen Energy 39 (24) (2014) 12784–12788.

[63] I. Nagase, T. Shimizu, The hydrogen absorbing properties of Ti-Cr-V alloys prepared by levitation melting method, Denki-Seiko (Electr. Furn. Steel) 74 (4) (2003) 233–239, https://doi.org/10.4262/denkiseiko.74.233.

[64] G.-J. Yang, X.-K. Suo, G.-R. Li, Introduction to advanced micro-nano coating materials and thermal spray, Advanced Nanomaterials and Coatings by Thermal Spray, Elsevier 2019, pp. 1–11, https://doi.org/10.1016/b978-0-12-813870-0.00001-2.

[65] M. Kazemipour, H. Salimijazi, A. Saidi, A. Saatchi, J. Mostaghimi, L. Pershin, A. Aref Arjmand, The electrochemical hydrogen storage properties of $Ti_{0.72}Zr_{0.28}Mn_{1.6}V_{0.4}$ alloy synthesized by vacuum plasma spraying and vacuum copper boat induction melting: a comparative study, Int. J. Hydrogen Energy 40 (2015) 15569–15577.

[66] L.-C. Zhang, Y. Liu, S. Li, Y. Hao, Additive manufacturing of titanium alloys by electron beam melting: a review, Adv. Eng. Mater. 20 (2018) 1700842, https://doi.org/10.1002/adem.201700842.

[67] L.-C. Zhang, L.-Y. Chen, A review on biomedical titanium alloys: recent progress and prospect, Adv. Eng. Mater. 21 (2019) 1801215, https://doi.org/10.1002/adem.201801215.

[68] G. Mandil, V.T. Le, H. Paris, M. Suard, Building new entities from existing titanium part by electron beam melting: microstructures and mechanical properties, Int. J. Adv. Manuf. Technol. 85 (5–8) (2015) 1835–1846, https://doi.org/10.1007/s00170-015-8049-3.

[69] C.D. Rabadia, Y.J. Liu, L. Wang, H. Suna, L.C. Zhang, Laves phase precipitation in Ti-Zr-Fe-Cr alloys with high strength and large plasticity, Mater. Des. 154 (2018) 228–238.

[70] C.D. Rabadia, Y.J. Liu, G.H. Cao, Y.H. Li, C.W. Zhang, T.B. Sercombe, H. Sun, L.C. Zhang, High-strength β stabilized Ti-Nb-Fe-Cr alloys with large plasticity, Mater. Sci. Eng. A 732 (2018) 368–377.

[71] R.L. Neto, T.P. Duarte, J.L. Alves, T.G. Barrigana, The influence of face coat material on reactivity and fluidity of the Ti6Al4V and TiAl alloys during investment casting, Proc IMechE Part L: J. Mater. Design Appl. 231 (1–2) (2017) 38–48, https://doi.org/10.1177/1464420716681824.

[72] T.B. Massalski (Ed.), Binary Alloy Phase Diagrams, second ed.ASM International, Materials Park, Ohio, 1990.

[73] T. Tetsui, Development of a TiAl turbocharger for passenger vehicles, Mater. Sci. Eng. A 329–331 (2002) 582–588.

[74] W. Shouren, G. Peiquan, Y. Liying, Centrifugal precision cast TiAl turbocharger wheel using ceramic mold, J. Mater. Process. Technol. 204 (1–3) (2008) 492–497.

[75] W.F. Cui, C.M. Liu, V. Bauer, H.J. Christ, Thermomechanical fatigue behaviours of a third generation γ-TiAl based alloy, Intermetallics 15 (5–6) (2007) 675–678.

[76] F. Gomes, J. Barbosa, C.S. Ribeiro, Induction melting of γ-TiAl in CaO crucibles, Intermetallics 16 (11–12) (2008) 1292–1297.

[77] J. Wang, K. Yang, N. Liu, L. Jia, G.Y. Yang, H.P. Tang, Microstructure and tensile properties of Ti-48Al-2Cr-2Nb rods additively manufactured by selective electron beam melting, J. Miner. Met. Mater. Soc. 69 (2017) 2751–2756, https://doi.org/10.1007/s11837-017-2583-4.

[78] J.M. Liang, L. Cao, Y.H. Xie, Y. Zhou, Y.F. Luo, K.Q. Mudi, H.Y. Gao, J. Wang, Microstructure and mechanical properties of Ti-48Al-2Cr-2Nb alloy joints produced by transient liquid phase bonding using spark plasma sintering, Mater. Char. 147 (2019) 116–126.

[79] S.J. Qu, S.Q. Tang, A.H. Feng, C. Feng, J. Shen, D.L. Chen, Microstructural evolution and high-temperature oxidation mechanisms of a titanium aluminide based alloy, Acta Mater. 148 (2018) 300–310.

[80] N. Eliaz, D. Eliezer, D.L. Olson, Hydrogen-assisted processing of materials, Mater. Sci. Eng. A289 (2000) 41–53.

[81] V.N. Fokin, E.E. Fokina, V.I. Torbov, B.P. Tarasov, S.P. Shilkin, R.A. Andrievskii, Hydriding behavior of spherical particles of a titanium–aluminum–tin alloy, Inorg. Mater. 42 (3) (2006) 261–263, https://doi.org/10.1134/S0020168506030095.

[82] V.N. Fokin, E.E. Fokina, B.P. Tarasov, Chemical transformations of TiAl and Ti_3Al intermetallides in ammonium medium, Russ. J. Gen. Chem. 78 (6) (2008) 1118–1122, https://doi.org/10.1134/S1070363208060029.

[83] V.N. Fokin, E.E. Fokina, I.I. Korobov, B.P. Tarasov, Investigation of $Ti_{1.5}Al$–NH_3 and Ti_2Al–NH_3 systems, Int. J. Hydrogen Energy 36 (2011) 1217–1221.

[84] J. Van Humbeeck, Non-medical applications of shape memory alloys, Mater. Sci. Eng. A 273–275 (1999) 134–148.

[85] K. Otsuka, X. Ren, Recent developments in the research of shape memory alloys, Intermetallics 7 (5) (1999) 511–528.

[86] T. Duerig, A. Pelton, D. Stöckel, An overview of nitinol medical applications, Mater. Sci. Eng. A 273–275 (1999) 149–160.

[87] T. Otsuka, K. Kakeshita, Science and technology of shape-memory alloys: new developments, MRS Bull. 27 (2) (2002) 91–100.

[88] W. Tang, B. Sundman, R. Sandström, C. Qiu, New modelling of the B2 phase and its associated martensitic transformation in the Ti-Ni system, Acta Mater. 47 (12) (1999) 3457–3468.

[89] J. Khalil-Allafi, A. Dlouhy, G. Eggeler, Ni_4Ti_3 -precipitation during aging of NiTi shape memory alloys and its influence on martensitic phase transformations, Acta Mater. 50 (17) (2002) 4255–4274.

[90] G. Sandrock, A panoramic overview of hydrogen storage alloys from a gas reaction point of view, J. Alloy. Comp. 293–295 (1999) 877–888.

[91] P. Dantzer, Properties of intermetallic compounds suitable for hydrogen storage applications, Mater. Sci. Eng. A 329–331 (2002) 313–320.

[92] B.P. Tarasov, M.V. Lototskii, Hydrogen energetics: past, present, prospects, Russ. J. Gen. Chem. 77 (4) (2007) 660–675, https://doi.org/10.1134/S1070363207040299.

[93] K.-H. Young, J. Nei, The current status of hydrogen storage alloy development for electrochemical applications, Materials 6 (10) (2013) 4574–4608.

[94] B.P. Tarasov, E.E. Fokina, V.N. Fokin, Preparation of hydrides of intermetallic compounds, Russ. J. Gen. Chem. 84 (2) (2014) 194–197, https://doi.org/10.1134/S1070363214020054.

[95] M.V. Lototskyy, V.A. Yartys, B.G. Pollet, R.C. Bowman Jr., Metal hydride hydrogen compressors: a review, Int. J. Hydrogen Energy 39 (11) (2014) 5818–5851.

[96] N.A.A. Rusman, M. Dahari, A review on the current progress of metal hydrides material for solid-state hydrogen storage applications, Int. J. Hydrogen Energy 41 (28) (2016) 12108–12126.
[97] M. Williams, M.V. Lototsky, M.W. Davids, V. Linkov, V.A. Yartys, J.K. Solberg, Chemical surface modification for the improvement of the hydrogenation kinetics and poisoning resistance of TiFe, J. Alloy. Comp. 509S (2011) S770–S774.
[98] T. Kabutomori, H. Takeda, Y. Wakisaka, K. Ohnishi, Hydrogen absorption properties of Ti-Cr-A (A =V, Mo or other transition metal) B.C.C. solid solution alloys, J. Alloy. Comp. 231 (1995) 528–532.
[99] V. Dixit, J. Huot, Structural, microstructural and hydrogenation characteristics of Ti-V-Cr alloy with Zr-Ni addition, J. Alloys Comd. 776 (2019) 614–619.
[100] D. Mori, K. Hirose, N. Haraikawa, T. Takiguchi, T. Shinozawa, T. Matsunaga, K. Toh, K. Fujita, A. Kumano, H. Kubo, High-pressure Metal Hydride Tank for Fuel Cell Vehicles, *JSAE* 20077268.
[101] Y. Kojima, Hydrogen storage materials for hydrogen and energy carriers, Int. J. Hydrogen Energy 44 (2019) 18179.
[102] Y. Morita, T. Gamo, S. Kuranaka, Effects of nonmetal addition on hydriding properties for Ti–Mn Laves phase alloys, J. Alloy. Comp. 253–254 (1997) 29–33.
[103] M.W. Davids, M. Lototskyy, Influence of oxygen introduced in TiFe-based hydride forming alloy on its morphology, structural and hydrogen sorption properties, Int. J. Hydrogen Energy 37 (23) (2012) 18155–18162.
[104] V.N. Fokin, E.E. Fokina, I.I. Korobov, B.P. Tarasov, Chemical interaction between TiFe and ammonia, Inorg. Mater. 44 (2) (2008) 142–145, https://doi.org/10.1134/S0020168508020118.
[105] V.N. Fokin, E.E. Fokina, I.I. Korobov, B.P. Tarasov, Hydriding of intermetallic compound Ti_2Ni, Russ. J. Inorg. Chem. 59 (10) (2014) 1073–1076, https://doi.org/10.1134/S0036023614100076.
[106] V.N. Fokin, E.E. Fokina, I.I. Korobov, B.P. Tarasov, Phase transformations in the systems $Ti_2Fe–H_2$ and $Ti_2Fe–NH_3$, Russ. J. Inorg. Chem. 61 (7) (2016) 891–895, https://doi.org/10.1134/S0036023616070044.
[107] A.A. Volodin, R.V. Denys, C. Wan, I.D. Wijayanti, S. Suwarno, B.P. Tarasov, V.E. Antonov, V.A. Yartys, Study of hydrogen storage and electrochemical properties of AB_2-type $Ti_{0.15}Zr_{0.85}La_{0.03}Ni_{1.2}Mn_{0.7}V_{0.12}Fe_{0.12}$ alloy, J. Alloy. Comp. 793 (2019) 564–575.
[108] F. Hu, Y.-G. Chen, C.-L. Wu, J.-J. Zhou, Melting processes and performance improvement of kilogram-grade V-based BCC hydrogen storage alloy, J. Funct. Mater. 42 (4) (2011) 708–710.
[109] R. Fichte, H.-J. Retelsdorf, P.K. Künert, Method of making a titanium-containing hydrogen storage alloy, US patent 4643874 (1987).
[110] A. Kostov, B. Friedrich, Predicting thermodynamic stability of crucible oxides in molten titanium and titanium alloys, Comput. Mater. Sci. 38 (2) (2006) 374–385.
[111] J. Lapin, Z. Gabalcová, T. Pelachová, Effect of Y_2O_3 crucible on contamination of directionally solidified intermetallic Ti-46Al-8Nb alloy, Intermetallics 19 (3) (2011) 396–403.
[112] H. Zhang, M. Gao, R. Cui, L. Ma, H. Zhang, X. Tang, Physical erosion of yttria crucibles in Ti-54Al alloy casting process, J. Mater. Process. Technol. 211 (12) (2011) 2004–2011.
[113] C. Renjie, G. Ming, Z. Hu, G. Shengkai, Interactions between TiAl alloys and yttria refractory material in casting process, J. Mater. Process. Technol. 210 (9) (2010) 1190–1196.
[114] V.H. López, A.R. Kennedy, Flux-assisted wetting and spreading of Al on TiC, J. Colloid Interface Sci. 298 (1) (2006) 356–362.
[115] K. Liu, Y.C. Ma, M. Gao, G.B. Rao, Y.Y. Li, K. Wei, X. Wu, M.H. Loretto, Single step centrifugal casting TiAl automotive valves, Intermetallics 13 (9) (2005) 925–928.
[116] H. Zhang, X. Tang, C. Zhou, H. Zhang, S. Zhang, Comparison of directional solidification of γ-TiAl alloys in conventional Al_2O_3 and novel Y_2O_3-coated Al_2O_3 crucibles, J. Eur. Ceram. Soc. 33 (5) (2013) 925–934.
[117] D. Eatesami, M.M. Hadavi, A. Habibollahzade, Melting of γ-TiAl in the alumina crucible, Russ. J. Non-Ferrous Metals 50 (4) (2009) 363–367.
[118] R.J. Cui, X.X. Tang, M. Gao, H. Zhang, S.K. Gong, Microstructure and composition of cast Ti-47Al-2Cr-2Nb alloys produced by yttria crucibles, Mater. Sci. Eng. A 541 (2012) 14–21.
[119] J.C. Schuster, M. Palm, Reassessment of the binary aluminum-titanium phase diagram, J. Phase Equilibria Diffusion 27 (3) (2006) 255–277.
[120] J. Barbosa, C. Ribeiro, C. Monteiro, Processing of gammaTiAl, by ceramic crucible induction melting, and pouring in ceramic shells, Mater. Sci. Forum 426–432 (2003) 1933–1938.
[121] J. Barbosa, H. Puga, C.S. Ribeiro, O.M.N.D. Teodoro, A.C. Monteiro, Characterisation of metal/mould interface on investment casting of γ-TiAl, Int. J. Cast Met. Res. 19 (6) (2006) 331–338.
[122] J. Barbosa, C.S. Ribeiro, O.M.N.D. Teodoro, C. Monteiro, Evaluation of Y_2O_3 front layer of ceramic crucibles for vacuum induction melting of TiAl based alloys, EPD Congr. 2005, Proc. Sess. Symp. TMS Annual Meeting, TMS, Warrendale, PA 2005, pp. 573–584.
[123] C.H. Li, Y.H. Gao, X.G. Lu, W.Z. Ding, Z.M. Ren, K. Deng, Interaction between the ceramic $CaZrO_3$ and the melt of titanium alloys, Advances in Science and Technology, vol. 70, , Trans Tech Publ, 2010 136–140.
[124] U.E. Klotz, C. Legner, F. Bulling, L. Freitag, C. Faßauer, S. Schafföner, C.G. Aneziris, Investment casting of titanium alloys with calcium zirconate moulds and crucibles, Int. J. Adv. Manuf. Technol. (2019) 1–11, https://doi.org/10.1007/s00170-019-03538-z.
[125] M.-W. Lu, K.-L. Lin, C.-C. Lin, Effect of the alumina content on the interfacial reactions between titanium and calcia/zirconia/alumina composites, Contributed Papers from Materials Science and Technology 2017 (MS&T17), 2017https://doi.org/10.7449/2017/MST_2017_1349_1356 , October 8-12-Pittsburgh, Pennsylvania USA.
[126] G. Chen, J. Kang, P. Gao, Z. Qin, X. Lu, C. Li, Dissolution of $BaZrO_3$ refractory in titanium melt, Int. J. Appl. Ceram. Technol. 15 (6) (2018) 1459–1466.
[127] Z. Zhang, K.L. Zhu, L.J. Liu, X.G. Lu, G.X. Wu, C.H. Li, Preparation of $BaZrO_3$ crucible and its interfacial reaction with molten titanium alloys, J. Chin. Cream. Soc. 41 (2013) 1272–1283.
[128] G. Chen, J. Kang, B. Lan, P. Gao, X. Lu, C. Li, Evaluation of Ca-doped $BaZrO_3$ as the crucible refractory for melting TiAl alloys, Ceram. Int. 44 (11) (2018) 12627–12633.
[129] T. Cegan, I. Szurman, M. Kursa, J. Holešinský, J. Vontorová, Preparation of TiAl-based alloys by induction melting in graphite crucibles, Met. Mater. 53 (2) (2016) 69–78.
[130] J. Otubo, O.D. Rigo, C.M. Neto, P.R. Mei, The effects of vacuum induction melting and electron beam melting techniques on the purity of NiTi shape memory alloys, Mater. Sci. Eng. A 438–440 (2006) 679–682.
[131] Z. Zhang, J. Frenzel, K. Neuking, G. Eggeler, On the reaction between NiTi melts and crucible graphite during vacuum induction melting of NiTi shape memory alloys, Acta Mater. 53 (14) (2005) 3971–3985.
[132] M. Moshref-Javadi, M. Belbasi, S.H. Seyedein, M.T. Salehi, Fabrication of (Ti,Hf)-rich NiTiHf alloy using graphitic mold and crucible, J. Mater. Sci. Technol. 30 (3) (2014) 280–284.
[133] I. Szurman, M. Kursa, Methods for Ni-Ti based alloys preparation and their comparison, Ostrava, Czech Republic METAL 2010 - 19th International Conference on Metallurgy and Materials 2010, pp. 861–866 , Conference Proceedings.
[134] G.M. Kramer, A comparison of chemistry and inclusion distribution and morphology versus melting method of NiTi alloys, J. Mater. Eng. Perform. 18 (5–6) (2009) 479–483.
[135] A. Kostov, B. Friedrich, Selection of crucible oxides in molten titanium and titanium aluminum alloys by thermo-chemistry calculations, J. Min. Met. 41 B (2005) 113–125.
[136] I.S. Kulikov, Thermodynamics of Oxides, “Metallurgia” Publ., Moscow, 1986 (in Russian).
[137] S.M. Howard, Ellingham Diagrams, http://showard.sdsmt.edu/MET320/Handouts/EllinghamDiagrams/Ellingham_v22_Macro.pdf 2006.
[138] P. Stratton, Ellingham diagrams – their use and misuse, Int. Heat Treat. Surf. Eng. 7 (2) (2013) 70–73, https://doi.org/10.1179/1749514813Z.00000000053.
[139] V.A. Yartys, I.Yu Zavaliy, M.V. Lototsky, A.B. Riabov, YuF. Shmalko, Oxygen-, boron- and nitrogen-containing zirconium-vanadium alloys as hydrogen getters with enhanced properties, Z. Phys. Chem. 183 (1994) 485–489.
[140] I.Yu Zavaliy, M.V. Lototsky, A.B. Riabov, V.A. Yartys, Oxide-modified Zr–Fe alloys: thermodynamic calculations, X-ray analysis and hydrogen absorption properties, J. Alloy. Comp. 219 (1–2) (1995) 38–40.
[141] J. Zhu, A. Kamiya, T. Yamada, W. Shi, K. Naganuma, K. Mukai, Surface tension, wettability and reactivity of molten titanium in Ti/yttria-stabilized zirconia system, Mater. Sci. Eng. A 327 (2) (2002) 117–127.
[142] X. Cheng, X.D. Sun, C. Yuan, N.R. Green, P.A. Withey, An investigation of a TiAlO based refractory slurry face coat system for the investment casting of Ti-Al alloys, Intermetallics 29 (2012) 61–69.
[143] X. Cheng, C. Yuan, N. Green, P. Withey, Evaluation of the inertness of investment casting molds using both sessile drop and centrifugal casting methods, Metall. Mater. Trans. A 44 (2) (2013) 888–898.
[144] X. Cheng, C. Yuan, D. Shevchenko, P. Withey, The influence of mould pre-heat temperature and casting size on the interaction between a Ti-46Al-8Nb-1B alloy and the mould comprising an Al_2O_3 face coat, Mater. Chem. Phys. 146 (3) (2014) 295–302.
[145] K. Li, D. Wang, H. Chen, L. Guo, Normalized evaluation of thermal shock resistance for ceramic materials, J. Adv. Ceram. 3 (3) (2014) 250–258.
[146] M.R. Izadpanah, A.R.A. Dezfoli, Prediction of the thermal shock resistance of refractory materials using R values, Mater. Sci. Poland 27 (2) (2009) 131–140.
[147] H. Zhang, X. Tang, C. Zhou, H. Zhang, S. Zhang, Comparison of directional solidification of γ-TiAl alloys in conventional Al_2O_3 and novel Y_2O_3-coated Al_2O_3 crucibles, J. Eur. Ceram. Soc. 33 (5) (2013) 925–934.
[148] F. Smeacetto, M. Salvo, M. Ferraris, Protective coatings for induction casting of titanium, Surf. Coat. Technol. 201 (24) (2007) 9541–9548.
[149] Y. Harada, T. Teratani, Y2O3 Spray-Coated Member and Production Method Thereof, 2009 U.S. Patent 7494723 B2.
[150] D. Camel, B. Drevet, V. Briz, F. Disdier, E. Cierniak, N. Eustathopoulos, The crucible/silicon interface in directional solidification of photovoltaic silicon, Acta Mater. 129 (2017) 415–427.
[151] J.T. Carleton, Graphite Crucible Test Method, U.S. Patent, 1969 3592047.
[152] S. Schaffoner, C.G. Aneziris, H. Berek, B. Rotmann, B. Friedrich, Investigating the corrosion resistance of calcium zirconate in contact with titanium alloy melts, J. Eur. Ceram. Soc. 35 (2015) 259–266.
[153] J. He, C. Wei, M.Y. Li, H.B. Wang, X.G. Lu, C.H. Li, Interface reaction between $BaZrO_3$ refractory and melted TiAl alloys, Trans. Nonferrous Metals Soc. China 6 (2015) 1505–1511.
[154] C.H. Li, H. Zhou, G.Y. Chen, R.M. Hu, Z. Wu, Z.L. Li, Preparation of TiFe based alloys melted by $BaZrO_3$ crucible and its hydrogen storage properties, J. Chongqing Univ. 39 (2016) 107–113.
[155] J. He, C. Wei, S. Wang, D. Meng, X. Lu, H. Wang, C. Li, $BaZrO_3$ refractory applied to the directional solidification of TiAl alloys, IOP Conf. Series: Mater. Sci. Eng., Vol. 117, 2016, 012033. https://doi.org/10.1088/1757-899X/117/1/012033.
[156] C. Wang, X. Xu, H. Yu, Y. Wen, K. Zhao, A study of the solid electrolyte Y_2O_3_doped $CaZrO_3$, Solid State Ion. 28 (1988) 542–545.
[157] M. Jiang, C. Li, X. Lu, B. Yang, W. Zhang, G. Tan, N. Gui, G. Wu, Z. Wu, Z. Li, Process for Vacuum Induction Melting of Titaniferous Hydrogen Storage Alloy by Using CaZrO3 Refractory Material, Patent CN102965528A.

[158] M. Jiang, W. Zhang, Z. Li, X. Lu, B. Yang, N. Gui, G. Tan, G. Wu, Z. Wu, Z. Li, Method for Smelting Hydrogen Storage Alloy Containing Titanium from $BaZrO_3$ Refractory Material by Vacuum Induction, Patent CN201210499696.8B.
[159] Z. Zhang, K. Zhu, L. Liu, X. Lu, G. Wu, G. Chen, Preparation of $BaZrO_3$ crucible and its interfacial reaction with molten titanium alloys, J. Chin. Ceram. Soc. 41 (9) (2013) 1278–1283, https://doi.org/10.7521/j.issn.0454–5648.2013.09.18.
[160] G. Chen, B. Li, P. Gao, W. Ali, Z. Qin, X. Lu, C.H. Li, Effect of CaO on preparation of $BaZrO_3$ crucible and its interfacial reaction to titanium alloy, J. Chin. Ceram. Soc. 9 (2017) 76, https://doi.org/10.14062/j.issn.0454-5648.2017.09.19.
[161] G. Chen, J. Kang, P. Gao, W. Ali, Z. Qin, X. Lu, C. Li, Effect of CaO additive on the interfacial reaction between the $BaZrO_3$ refractory and titanium enrichment melt, in: H. Kim, B. Wesstrom, S. Alam, T. Ouchi, G. Azimi, N.R. Neelameggham, S. Wang, X. Guan (Eds.), Rare Metal Technology 2018, the Minerals, Metals & Materials Series, Springer Int. Publ. 2018, pp. 235–244, https://doi.org/10.1007/978-3-319-72350-1_22.
[162] Z. Cheng, F. Meng, G. Chen, Z. Li, X. Lu, C. Li, Interface reaction between Y_2O_3 doped $BaZrO_3$ and TiNi melt, in: S.J. Ikhmayies, B. Li, J.S. Carpenter, J.-Y. Hwang, S.N. Monteiro, J. Li, D. Firrao, M. Zhang, Z. Peng, J.P. Escobedo-Diaz, C. Bai (Eds.), Characterization of Minerals, Metals, and Materials 2016, Springer, Cham 2016, pp. 737–744, https://doi.org/10.1007/978-3-319-48210-1_93.
[163] L.-H. Zhou, G.-Y. Chen, B.-T. Li, Z.-W. Cheng, W. Ali, X.-G. Lu, C.-H. Li, Microstructure evolution of Y_2O_3-doped $BaZrO_3$ and its compatibility with titanium melt, Chin. J. Nonferrous Metals 11 (2017) 49, https://doi.org/10.19476/j.ysxb.1004.0609.2017.11.12.
[164] C. Li, M. Li, H. Zhang, W. Ali, Z. Qin, H. Wang, X. Lu, Fabrication of Y_2O_3 doped $BaZrO_3$ coating on Al_2O_3 applied to solidification of titanium alloy, Surf. Coat. Technol. 320 (2017) 146–152.
[165] P. Zeik, K.L., Koss, D.A., Anderson, I.E. Howell, Microstructural evolution and thermal stability, Metall. Trans. A 23 (8) (1992) 2159–2167.
[166] N. Alangi, J. Mukherjee, P. Anupama, M.K. Verma, Y. Chakravarthy, P.V.A. Padmanabhan, A.K. Das, L.M. Gantayet, Liquid uranium corrosion studies of protective yttria coatings on tantalum substrate, J. Nucl. Mater. 410 (1–3) (2011) 39–45.
[167] J. Sure, M. Mishra, M. Tarini, A.R. Shankar, N.G. Krishna, P. Kuppusami, C. Mallika, U.K. Mudali, Microstructural characterization and chemical compatibility of pulsed laser deposited yttria coatings on high density graphite, Thin Solid Films 544 (2013) 218–223.
[168] J.W. Koger, C.E. Holcombe, J.G. Banker, Coatings on graphite crucibles used in melting uranium, Thin Solid Films 39 (1976) 297–303.
[169] J.B. Condon, C.E. Holcombe Jr., Crucible Materials to Contain Molten Uranium, Union Carbide Corp. – Nuclear Division, Oak Ridge Y-12 Plant, 1977, Report Y-2084 https://inis.iaea.org/search/search.aspx?orig_q=RN:9362354.
[170] B.R. Westphal, K.C. Marsden, J.C. Price, Development of a ceramic-lined crucible for the separation of salt from uranium, Metall. Mater. Trans. A 40 (2009) 2861–2866.
[171] J. Sure, A. Ravi Shankar, S. Ramya, U. Kamachi Mudali, Molten salt corrosion of high density graphite and partially stabilized zirconia coated high density graphite in molten LiCl-KCl salt, Ceram. Int. 38 (4) (2012) 2803–2812.
[172] L. Chong-He, H. Jin, Z. Zhao, Y. Bo, L. Hai-Yan, L. Xiong-Gang, L. Zhi-Lin, W. Zhu, W. Hong-Bin, Preparation of TiFe based alloys melted by CaO crucible and its hydrogen storage properties, J. Alloy. Comp. 618 (2015) 679–684.
[173] B. Yang, K.-L. Zhu, X.-G. Lu, Z.-L. Li, Z. Wu, G.X. Wu, C.-H. Li, Preparation of TiFe based alloy melted by $CaZrO_3$ crucible and its hydrogen storage properties, Chin. J. Process Eng. 12 (5) (2012) 849–856.
[174] F. Meng, Z. Cheng, G. Chen, X. Lu, C. Li, Hydration resistance of Y_2O_3 doped CaO and its application to melting titanium alloys, in: S.J. Ikhmayies, B. Li, J.S. Carpenter, J.-Y. Hwang, S.N. Monteiro, J. Li, D. Firrao, M. Zhang, Z. Peng, J.P. Escobedo-Diaz, C. Bai (Eds.), Characterization of Minerals, Metals, and Materials 2016, Springer, Cham 2016, pp. 745–752, https://doi.org/10.1007/978-3-319-48210-1_94.